Phenomenology of Supersymmetry and Dark Matter

by

Faiqa Riaz

A dissertation submitted in partial fulfillment of the requirements

for the degree of Master of Science in physics

Supervised by

Dr. Rizwan Khalid

School of Natural Sciences

National University of Sciences and Technology

Islamabad, Pakistan

FORM TH-4

National University of Sciences & Technology

MASTER'S THESIS WORK

We hereby recommend that the dissertation prepared under our supervision by: Faiqa Riaz, Regn No. NUST201463639MSNS78114F Titled: Fine Tuning in the Constrained Minimal Supersymmetric Standard Model - Dark Matter be accepted in partial fulfillment of the requirements for the award of **MS** degree.

Examination Committee Members

1. Name: PROF. ASGHAR QADIR Signature: Asghar Qadir

2. Name: DR. MUHAMMAD ALI PARACHA Signature:

3. Name: Signature:

External Examiner: DR. ISHTIAQ AHMED Signature:

Supervisor's Name: DR. RIZWAN KHALID Signature:

Head of Department

14-03-18
Date

COUNTERSINGED

Date: 14-03-18

Dean/Principal

THESIS ACCEPTANCE CERTIFICATE

Certified that final copy of MS thesis written by **Ms. Faiqa Riaz**, (Registration No. **NUST201463639MSNS78114F**), of **School of Natural Sciences** has been vetted by undersigned, found complete in all respects as per NUST statutes/regulations, is free of plagiarism, errors, and mistakes and is accepted as partial fulfillment for award of MS/M.Phil degree. It is further certified that necessary amendments as pointed out by GEC members and external examiner of the scholar have also been incorporated in the said thesis.

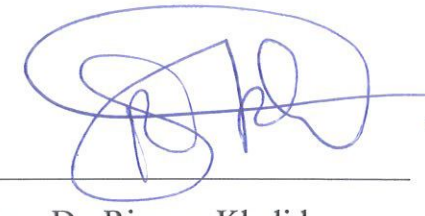

Signature: _____

Name of Supervisor: Dr. Rizwan Khalid

Date: 14-03-18

Signature (HoD): _____

Date: 14-03-18

Signature (Dean/Principal): _____

Date: 14-03-18

Dedicated to

My dear husband and parents

Acknowledgement

In the name of Allah (S.W.T), the most Merciful, the most Gracious. I want to thank Almighty Allah, Who bestowed on me His blessings and gave me such vision and strength to accomplish this work successfully.

I am deeply grateful to my supervisor Dr. Rizwan Khalid, Head of Department, SNS, for his guidance, cooperation and stimulating advices throughout my research work. Without his help it could have been very difficult to complete my dissertation successfully. I am also thankful to my GEC members Dr. Ali paracha and Dr. Asghar Qadir for their guidance and continuous encouragement throughout my research. I thank to all the faculty members of SNS Physics department for helping me throughout during my research and course work as well.

I express heartiest love and respect to my parents, who always supported me to educate myself with higher studies. Especially my father always stood by my side to go for unseen. Without their prayers and support I could not have done anything in my life. My husband, Dr. Muhammad Naveed has been a continuous encouragement and motivation throughout my work. Without his support i would have not been able to complete my research and course work.

I would also like to thank all of my class mates, especially Abeera and Daniyal for their support and helping hand, to PhD scholars Mureed Hussain and M. Usman Sharif for being readily available for discussions. Mureed has been very co-operative during my research work and always guided me whether it's computational problem or a theoretical one.

Abstract

In this thesis review is done of the paper, 'How Finely Tuned is Supersymmetric Dark Matter?', written by John Ellis (TH Division, CERN, Geneva, Switzerland) and Keith A. Olive (Theoretical Physics Institute, School of Physics and Astronomy, University of Minnesota, USA) by considering constrained minimal supersymmetric standard model. The sensitivities of the neutralino dark matter relic density, $\Omega_\chi h^2$ are quantified by doing variations in input parameters of the said model. It is found that there are generic domains in the cMSSM parameter space where relic density falls within the preferred value of relic abundance measured by Cosmology. The regions like 'Focus-Point' region, 'Funnel' region and the regions where there is dominant direct-channel pole annihilations, have sharp increase in the sensitivity to the input parameters. Funnel region is explored for high values of $\tan\beta$. The existence of radiative electroweak symmetry breaking region is also investigated for large and small values of top mass.

Contents

Chapter 1

Introduction

"*This is a tale of an elusive matter that I have chosen to relay in verse*;
It fills the stretches of empty space- one quarter of the universe!
It seems to be clumpy, slow-moving, dark and not the slightest bit rare.
In galaxies, in clusters and the spaces between - wherever you look, it's there!
How can we detect this elusive foe? We must journey underground.
With detectors at ultra-cool temperatures it may in the future be found.
But how to describe it? Just what is it? We must have a decent description!
Equipped with a theorist's trustworthy tools, we will find the right prescription.
A new model of physics may do the job, so we'll give each quark a twin!
We'll double the leptons and forces too, but each with different spin.
Now armed with code and computer power, we've gained a neat prediction.
If dark matter exists as a superpartner, it gives us a new direction:
We'll know what to look for and what to expect, and hopefully it'll come to pass,
That in the depths of detection chambers, we'll find dark matter at last!"

Sophie Underwood [1]

'Dark matter', as the name suggests, neither emits nor interacts with electromagnetic radiation. The visible world which we know, including stars, planets and cosmic dust abounds only 4 % of the energy density of the whole universe. About 26 % of the matter is said to be made up of this unseen matter and rest of about 75 % of the energy density, about which astronomers are not able to comprehend,

takes form of the 'dark energy'. Among these components, dark energy is the most mysterious component of all [2].

The fluctuations in density observed today could not have been established without the existence of dark matter, that is inferred from the cosmic microwave background (CMB). CMB is a background that fills the entire universe and is residual radiation of the hot Big Bang. In 1992, COBE (Cosmic Background Explorer) was the first satellite sent to study the cosmological fluctuations. Then in 2001, WMAP (Wilkinson Microwave Anisotropy Probe), a satellite borne experiment [3], was launched to study these fluctuations in more detail. And now Planck [4],[5] is the latest mission which was launched to help understand the origin and evolution of our universe with greater sensitivity and resolution.

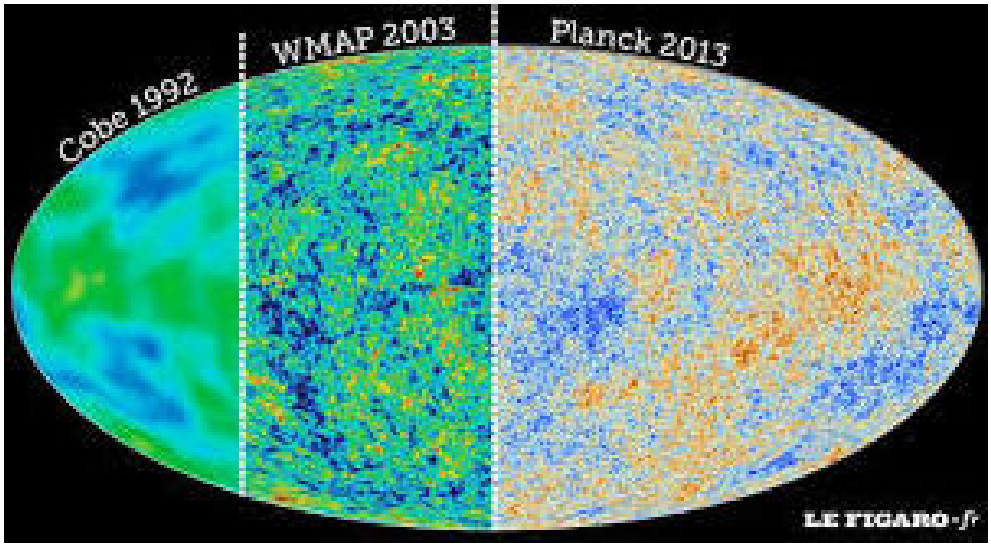

Figure 1.1: CMB temperature fluctuations: a comparison between COBE, WMAP and Planck. [6]

All the present fundamental models, for looking at dark matter, apply the standard idea of quantum field theory to illustrate the possible candidates [**?**],[8]. They can be categorized by the dark matter particle's spin and mass. The masses of hypothesized candidates stretch over a long span of mass, as depicted in Table 1.1

In search of dark matter candidate supersymmetric model is considered, as the general relativity is combined with the quantum field theory, we are lead to the

Table 1.1: Characteristics of Dark Matter Candidates

Type	Particle Spin	Approximate Mass Range
Axion	0	μev- mev
Sterile Neutrino	1/2	kev
Inert Higgs Doublet	0	50 Gev
Neutralino	1/2	10 Gev-10 Tev
Kaluza-Klein UED	1	Tev

supersymmetric doubling of the particles. The theory is called Supersymmetry [9],[10]. The bosonic degrees of freedom which are integral-spin particles, are allied to fermionic degrees of freedom that are half-integral superpartners, and vice-versa. Sleptons and squarks, having spin 0 are the examples of superpartners of leptons and quarks, which are half-integral spin particles in the standard model. Neutralino is another example of supersymmetric particle, having spin half, and is Majorana particle (particles which are their own anti-particles), composed of linear combination of Z-ino, higgsino and photino (superpartners of Higgs boson, the neutral Z boson and photon respectively).

In a supersymmetric model, minimal supersymmetric standard model (discussed in chapter 3), the most appealing candidate of dark matter, the neutralino, is the lightest supersymmetric particle. It is kept stable by the presence of discrete symmetry i.e. R-parity that prevents it to decay further. While debating about supersymmetric models, the most important element is realizing about R-parity. This discrete symmetry is defined as; $R = -1^{3(B-L)+2S}$, where S defines spin and B and L defines baryon and lepton numbers. This means that partners and superpartners have opposite sign parity. If we do not have R-parity, then there is catastrophe i.e., whenever we turn on SUSY, there is rapid proton decay mediated through SUSY interactions. The conservation of R-parity has also great significance in supersymmetric theories regarding the existence of cold dark matter particle candidates, as without it, there would be no proper rules for preventing the SUSY particles from decaying down to the particles with masses of few Gev or larger. So the phenomenol-

ogy of R-parity [11],[12] renders the lightest supersymmetric particle stable. Thus SUSY proposes a viable stable candidate whose mass is even smaller than few Tev and interacts with ordinary matter through weak interactions. It is shown later that if such weakly interacting particle exists, then it's relic abundance may concur the cosmological abundance and it can be accounted for the dark matter problem.

With the help of appropriate parameters of a supersymmetric model (physics beyond the standard model), we are allowed to probe into the nature of possible dark matter candidates. The model of choice in this thesis is the Minimal Supersymmetric Standard Model (MSSM). This model abounds all the SM fields with an additional Higgs doublet (the reason is discussed in next Chapter) along with other supersymmetric partners to form multiplets. The gauge group (described in next chapter) of all the interactions of the fields uniquely specifies this model. The complex details in the MSSM shows up not at the supersymmetric level but at the point where the SUSY is broken. Supersymmetric Lagrangian in the MSSM is discussed in detail in [13], containing large number of parameters.

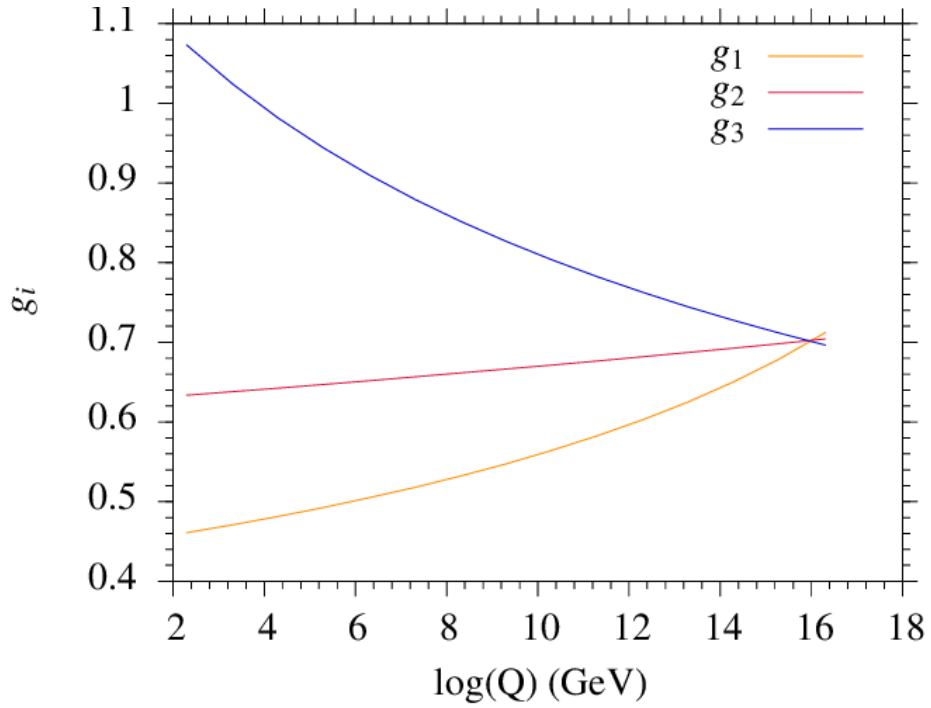

Figure 1.2: Gauge coupling unification in Supersymmetry

Further extension of the MSSM leads us to other scenarios of analyzing the spectrum of SUSY particles and their details. The appearance of MSSM is spoiled due to the existence of about 100 free parameters. If the breaking mechanism of SUSY is altogether unspecified, then the parameters are left free. Many SUSY models are studied and investigated, the research work of my dissertation is based upon constrained minimal supersymmetric standard model (cMSSM). This model functions in terms of 5 parameters described in chapter: 4.

In chapter 2, a review of standard model has been given along with it's successes and challenges to overcome. Then the dark matter is discussed in the light of cosmology and it's existence is explained through various evidences.

In chapter 3, the subject of supersymmetry is discussed and how it is able to render a plausible candidate for dark matter. Then minimal supersymmetric standard model is explained briefly.

In chapter: 4, constrained minimal supersymmetric standard model is explained along with all the Calculational details, where we will see hoe annihilations and co-annihilations (explained in chapter 4) can help us to get correct value of dark matter relic density. Last chapter concludes the review done in this thesis.

Chapter 2

Standard Model of Particle Physics and Introduction of Dark Matter

2.1 Standard Model of Particle Physics

The standard model (SM) of particle physics describes all the elementary particles and describes their interactions. The SM is a Lorentz invariant quantum field theory that is based on the group

$$SU(3)_c \times SU(2)_L \times U(1)_Y,^{1}$$

The subscript c of SU(3) denotes 'color' referring to the theory strong interactions theory, where the theory is called quantum chromodynamics (QCD). The eight gluons are the generators of this theory. The next part $SU(2)_L \times U(1)_Y$, together represents the electroweak interactions. The subscript L of $SU(2)$ indicates that only the left-handed particles take part in $SU(2)$ mediated interactions while the right-handed particles do not.[2] The group SU(2) has 3 generators which means this

[1] SU(N) represent the groups of $N \times N$ unitary matrices with determinant 1, and is given by $N^2 - 1$ real numbers. U(1) is a one dimensional group of rotations.

[2] Dirac representation of the Lorentz algebra is not irreducible. we write the irreducible representation in terms of Weyl fields, where the left and right-handed Weyl fields transform similarly

group has 3 massless gauge bosons that mediate the weak nuclear force. Finally, Y represents weak hypercharge. The weak hypercharge is adjusted to give the correct electromagnetic charges to the particles, when $SU(2)_L \times U(1)_Y$ is spontaneously broken down to $U(1)_{em}$, where 'em' refers to electromagnetism. The relationship between I_3, the third component of $SU(2)$ isospin, the hypercharge Y and the corresponding electric charge Q is given by Gell-Mann-Nishijima relation:

$$Q = I_3 + \frac{Y}{2}$$

We construct the gauge theory of the SM by specifying the gauge group. Then all the renormalizable terms that are invariant under the global gauge symmetry, can be written in the Lagrangian. However, it is very important that the theory follow the local gauge invariance, so that the interactions are invariant under the symmetry group for each particle individually. It can also be understood as the interactions of the particles belonging to the same multiplet of a symmetry group are same. The groups SU(N) can be represented by $N^2 - 1$ real numbers, so that adjoint of N representation is $N^2 - 1$ dimensional that contains all the massless fields. The SM, therefore, has 8 gluons, 3 bosons and 1 hypercharge. The Higgs field is responsible to give masses to all the massive particles through spontaneous symmetry breaking (SSB) [14],[15],[16],[17],[18] which refers to the breaking of electroweak unification.[3] Because of this symmetry breaking, we see two charged weak bosons and a neutral weak boson, that are all massive. And we can say that unification of electroweak force is broken down to electromagnetism. The symmetry is broken in such a way that Lagrangian of the theory is still invariant under the gauge group, but the ground state is not invariant providing us with massive fermions and appropriately massive gauge bosons. Finally, all the masses and couplings in the theory are renormalized so that we can relate the bare charges of the theory to the known data. It gives rise to the concept of "running ", which refers to the energy-dependent coupling constant that determines the strength of the force during an interaction.

under rotations but differently under Lorentz boost. This aspect of the theory is known as chirality.

[3]This unification of electroweak force led to the Nobel Prize in 1979.

Fermions All the elementary particles in the nature have been defined in the SM that are categorized in to fermions and bosons. (Fermions being spin half particles while bosons being integral spin particles).In the SM, the fermionic degrees of freedom refer to the elementary constituents that make up all the matter in nature. Elementary fermions are classified into quarks and leptons. There are three families or generations of the quarks and leptons. First generation is the lightest while third is the heaviest one. Table 2.1 shows the fermions present in the SM. Here τ, μ and e are the tau, muon and electron leptons where as ν_τ, ν_μ and ν_e are corresponding neutrinos. t, b, c, s, u and d are top, bottom, charm, strange, up and down quarks respectively. The anti-particles of these particles also exist and are a part of the SM. In the table, subscript R(L) refers to right(left) handed fermions. Due to chirality,

	Symbol	Particle		
Quarks	q_L^i	$\begin{pmatrix} u \\ d \end{pmatrix}_L$	$\begin{pmatrix} t \\ b \end{pmatrix}_L$	$\begin{pmatrix} c \\ s \end{pmatrix}_L$
	q_R^i	u_R	t_R	c_R
	d_R^i	d_R	b_R	s_R
Leptons	l_L^i	$\begin{pmatrix} \nu_e \\ e \end{pmatrix}_L$	$\begin{pmatrix} \nu_\mu \\ \mu \end{pmatrix}_L$	$\begin{pmatrix} \nu_\tau \\ \tau \end{pmatrix}_L$
	e_R^i	e_R	μ_R	τ_R

Table 2.1: Fermions in the SM

only the left-handed fermions transform as $SU(2)_L$ doublets, whilst the right-handed components, e_R, μ_R, τ_R e.t.c., are singlets under this group.[4]

Bosons The fundamental forces are mediated by the particles which are bosonic in nature. Mediating a force means, exchanging of a particle. For example a virtual photon is interchanged between two electrons interacting with each other, and hence they repel.

[4]From the point of view of $SU(2)_L$ invariance there is no difference between an electron and it's neutrino. $SU(2) \times U(1)$ is therefore, broken spontaneously to $U(1)_{em}$. Now the electron acquires the electric charge and the neutrino doesn't.

Gauge bosons in this model are listed in Table 2.2, where, the photon represented as γ, is massless and electrically neutral particle, have spin 1 and mediate the electromagnetic force. The $W^{\pm}$ bosons (electrically charged) and Z^0 boson (electrically neutral) are massive, having spin 1, mediate the electroweak force. The eight gluons, g_i (i=1,2....8) are massless having spin 1 and electrically neutral and are the mediators of strong force. They carry color-anticolor charge.

	Gauge boson	Symbol
Electromagnetic interactions	photon	γ
Weak interactions	W, Z bosons	$W^{\pm}$ Z
Strong interactions	gluon	g

Table 2.2: Gauge bosons in the SM

The eight gluons are the generators of strong force belonging to the sub group $SU(3)_c$, while $W^{\pm}$ and Z bosons interact through the $SU(2)_L$ weak group and the photon is the generator of $U(1)_{em}$ transformations.

Higgs Bosons The Higgs boson, a spin 0 particle and an SU(2) doublet, was discovered in 2012 at the Large Hadron Collider (LHC). Supersymmetry breaking (SSB) provides masses to all the massless particles through the Higgs mechanism. The symmetry group breaks as:

$$SU(2)_L \times U(1)_Y \rightarrow U(1)_{em}.$$

Because of this symmetry breaking, we end up with two massive charged bosons, W^+ and W^-, and two neutral bosons, among which Z is massive and the photon is massless. It is to be noted that the mass term $W_\mu W^\mu$ is not gauge invariant and therefore, not directly allowed in the Lagrangian.

The electron Dirac field operator may be divided into 'right-handed' and 'left-

handed' parts by substituting:

$$e = e_L + e_R,^{5}$$

here, $e_L(e_R)$ are the left(right)-handed chiral states and transform differently under boost.

The Dirac mass term for fermions, *i.e.* $\bar{\psi}_L\psi_R$ is not allowed in the Lagrangian as it is not gauge invariant, since ψ_L is an $SU(2)_L$ doublet whereas ψ_R is a singlet. This provokes the requirement of the massive fermions. Thus Higgs boson was postulated in order to give masses to all the fermions and the weak bosons through a process known as Higgs mechanism. Now a gauge invariant term can be written with the help of the Higgs field, which is also an $SU(2)_L$ doublet, just like ψ_L. This term is written as $\bar{\psi}_L\Phi\psi_R$ for a Higgs field Φ. The spontaneous symmetry breaking of $SU(2)_L \times U(1)_Y$ to $U(1)_{em}$ offers a non-zero vacuum expectation value to the Higgs boson and thus generating masses for the weak bosons and other quarks and leptons. These types of interactions, fermion-scalar-fermion, are known as Yukawa interactions.

As discussed before in the first chapter that the SM is still unable to open up the true nature of massive bulk of the universe named as Dark Matter. In the following chapter, the nature of dark matter and it's existence is discussed which ultimately leads to the supersymmetry and hence other supersymmetric models. (Models are discussed in next chapter).

2.2 Dark Matter

Dark matter is composed of 26.8% of the energy density of the universe and in comparison, only about 4% of the energy budget of the universe is consumed by matter that fits into the SM of particle physics, shown in Figure 2.1. Major portion of the universe is consumed by dark energy, whose features are discussed in section 2.2.2.

[5] where $e_L = \frac{1}{2}(1-\gamma_5)e$ and $e_R = \frac{1}{2}(1+\gamma_5)e$, with $\gamma^5 = \begin{pmatrix} -I_2 & 0 \\ 0 & I_2 \end{pmatrix}$.

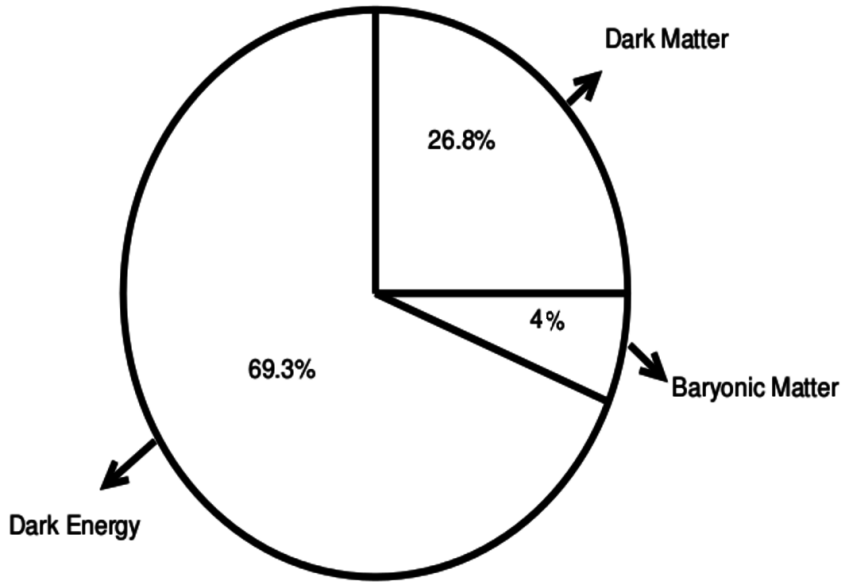

Figure 2.1: Energy Budget of the universe. [19]

2.2.1 Cosmic History Of Universe

The cosmic history of the universe is well described by the so-called standard model of cosmology, otherwise big bang theory . It abounds all the important features necessary to understand the nature of DM. The theory explains that in the beginning, there was an explosion which occurred simultaneously everywhere and every particle rushed away from every other particle. At the time, $t = 1/100$ s, the temperature of the universe was so hot ($10^{11}{}^{\circ}C$) that no components of ordinary matter or molecules could held together to form the structures seen today and the universe was a boiling and bright, blinding fog of radiation. At this time, the most abundant particles were electrons, positrons, neutrinos and photons. These particles readily annihilated to each other and were also created equally. The energetic photons, for example, scattered off each other to create matter particles and their anti-particles. Also these particle-antiparticle pairs annihilated into each other to produce photons. At this temperature of hundred thousand million degrees, there was also a contamination of heavier particles like protons and neutrons, where this number was one proton and one neutron for every one thousand million of the abundant particles in

the early universe.

The temperature continued to drop further, reaching 10,000 million degrees at $t = 1s$ and 3000 million degrees after about $t = 14s$ [20]. Now the creation rate of the particles slowed down as the photons were not energetic enough to produce protons and neutrons, but still they had energy to produce electrons. In a while, the protons and the neutrons decreased in number by annihilating with their respective anti-particles. The photons too lose the energy even to create an electro-positron pair. So the recreation of particles was suppressed as the universe cooled down. Since, not all the particles were annihilated with their anti-particles, so there was some excess of particles over anti-particles.

Now as the temperature continued to drop, the protons and neutrons joined together to form complex nuclei like that of hydrogen and helium after about 100s after the Big Bang. At the end of three minutes, there was small amount of nuclear material left along with small number of electrons after electron-positron annihilation. After that the matter continued to rush apart and about few hundred thousand years later, electrons were cool enough to join the hydrogen/helium nuclei to form atoms. At this time, the number density of the particles reached 'freeze-out' level. Other elements like lithium, beryllium and boron were also formed at this stage but not too many of the heavy elements formed. The resulting gas began to form clumps under the influence of gravity, which ultimately condensed into galaxies and stars of the present time.

Cosmic Microwave Background

When the matter and radiation decoupled, large-scale structure formation took place and thus the paths of the suddenly liberated photons become essentially straight lines. These photons swarm like a uniform background of microwaves over the entire sky and are known as the cosmic microwave background (CMB). For the past few decades, CMB has been considered as an accurate tool to understand the origin of the universe. This background radiation was discovered in 1955, by Arno Penzias and Robert Wilson and was predicted in Big Bang theory. In 1992, Cosmic Background Explorer (COBE) satellite made the observations in the fluctuations of CMB. These fluctuations were the translating evidence for the irregularities in

the matter's density and it's distribution in the early universe. Various independent high resolution observations have been made after the discovery due to COBE, but the view of CMB has become more sharpened and improved with the discovery of WMAP.

In 2001, Wilkinson Microwave Anisotropy Probe (WMAP) [21], [22] was launched to further pin down the free parameters offered by the big bang model. The structure of the universe has been explained by the relative intensity of the CMB at the time time of decoupling of matter and radiation. For example, the regions with larger content of the matter will experience greater gravity and hence the photons leaving this region will have greater pull upon them. Thus on the average these photons will appear fainter or less energetic. So we can say that at larger scales, the variation in the study of CMB provides the prediction of the distribution of DM in the universe at the time of decoupling.

However, Planck [4],[5],[23] is the latest mission launched to understand the origin and evolution of the universe, by studying CMB, with greater sensitivity and resolution.

Hot DM vs Cold DM

Hot dark matter (HDM) refers to the particles that move very fast and therefore, do not clump with baryonic matter and spreads around the universe. At redshift of about 10^6 (time about one year after the big bang), the temperature of the universe was so hot (at T $\sim$ 3 $\times 10^2$ eV) and the HDM particles were moving so fast that they could not accumulate to the clumps of the sizes first seen by COBE. HDM is assumed to be comprised of particles that moved with ultra-relativistic velocities, like neutrinos. Neutrinos form hot DM and is discussed in section 2.2.2. The high speeds of these fast moving, hot particles cannot allow the small density fluctuations to clump together to create large fluctuations on galactic scales. Small initial fluctuations at the time of early universe caused the distribution of the matter in the universe. But considering a hot dark matter candidate, these fluctuations could be smoothed out due to the high speeds. Thus, hot dark matter theory is not well supported for the formation of galaxies and other stuff in the universe [24],[25].

On the other hand, CDM provides a better way of understanding how inhomogeneities are properly developed into the large-scale structures of today. The existence of CDM also agrees well with the observations of CMB made by Planck. By definition, CDM moved slower than the HDM, and at the time of structure formation, it was moving slow enough to be caught up by the gravitational puddles generated by the baryonic matter. At the time of freeze-out, the HDM particles have their mass less than kinetic energy and hence they are extremely relativistic. They are generally lighter in mass. While CDM particles have their mass greater than the temperature of the universe at the time of freeze-out, and hence they were non-relativistic. Their mass is generally heavier than the HDM particles.

By the end of this discussion, we are able to establish the fundamentals to understand the distribution of the relic abundance in the universe, which leads to 4% baryonic content and 26.8% CDM content of the universe depicted in Figure 2.1. The details of calculations are given in next section.

2.2.2 Energy Budget of the Universe

Since the universe is expanding as a result of Big Bang, there has been a tug-of-war between this expansion and the universe's self gravitation. If the universe is supposed to contain too little mass, it will continue to expand forever, and if it contains too much mass then it will collapse in on itself once again. Keeping a balance between expansion and gravitation for these two extremes, we define 'critical density'. Critical density is the quantity of mass which is needed to suspend the expansion of the universe at some infinitely distant time in the future.

The total relic density of the universe Ω

Since the large scale structures generated by the density perturbations in cosmology play an important role in the formation of the universe and estimating the overall density of the gravitating matter. Ω represents the common unit for the measurement of the density of matter and energy in the universe. Ω=1 represents 'critical density'. $\Omega > 1$ means, the universe will not only stop expanding but it will start collapsing, forming a 'closed' universe. But due to the phenomenon of

energy density that produces an anti gravity effect, the case $\Omega > 1$ is improbable. $\Omega < 1$ means that the expansion of the universe will continue forever and will make an 'open' universe. However, if $\Omega = 1$, then the universe is at the critical density forming a 'flat' universe. When the universe is at critical density, the universe will expand precisely at the right rate and will not collapse. Thus total density of the universe is written as:

$$\Omega = \frac{\rho}{\rho_c} = 1.$$

The total content of the matter only adds up to a fraction (about 0.268) of this critical density. Hence the dominant force in the universe is not that of matter. The existence of flat universe is also well supported by WMAP data. The total relic abundance, containing energy and matter, is constrained by WMAP as $\Omega_{tot} = 1.02 \pm 0.02$ [26],[27]. It means that the universe is maintained at the critical density ρ_c, pointing towards the flat universe,

Two parameters of cosmology circumscribe almost total density of matter in the universe. First is Ω_m, the total matter content of the universe, constituting 30.8 %. In this percentage only 17 % represents the baryonic abundance, Ω_b, while rest of it comprises cold DM, $\Omega_{CDM} = 26.8\%$. Second is Ω_Λ, the cosmological constant which is defined as the energy of vacuum of the space, responsible for covering 69.3 % of the universe's content shown in Figure 2.1.

Ω_b In The Present Age

In cosmology, there are several models incorporating particular set of parameters, to find constraints on the total energy density of the universe, the physical density of baryons and the density of cold dark matter [28],[29][30]. The accepted values of these parameters keep on changing as latest and updated observations become available. The direct measurements, from WMAP and Planck satellites, of the CMB spectrum makes most of the observational cosmology. The results based on full-mission Planck observations of the CMB radiations [5] presents the value of Ω_m as:

$$\Omega_m = 0.308 \pm 0.012.$$

The baryon abundance, Ω_b can be measured by adding up all the baryonic contributions that we can see. But while making measurements at large scale we get into trouble because of unknown distances and age scale of the universe. Since it has been observed that for greater distances of the galaxy, it's spectral lines are more redshifted because of expansion of the universe. This measurement scale is more convenient than considering the exact age of the universe. Joining this idea with the fact that look-back time of the universe is greater for distant galaxies and thus different epochs in the history could be explained with the help of different amounts of redshifts. For example, nearby objects are seen at zero redshift, while the Coma Cluster lies at the redshift of about 0.02. For distant objects whose spectral lines are shifted by 300 %, that is, for redshift = 3, we can well examine the past baryonic density of the universe.

Presently, at zero redshift, baryons are mostly found in stars inside galaxy and gas from the groups of galaxies. The most important measurement of Ω_b is made by WMAP whose main objective was to establish the parameters of big bang. It provided us with high-precision cosmology and most importantly the value of baryonic density, i.e., 0.044 ± 0.004 [26]. Analyzing all the estimates of Ω_b from different resources, we can say that prediction of Ω_b from big bang nucleosynthesis is 0.04, at zero redshift it is 0.021, at redshift = 3 Ω_b = 0.04 and from WMAP result Ω_b = 0.044. These results point towards the fact that more or less there are no major discrepancies and the baryonic abundance is inferred to be 0.04.

However, there might be some unseen baryonic matter as well, since the visible universe does not account for the baryonic density suggested by the recent Planck measurements [23]. In the massive clusters, the fraction of the observed baryons is 15% for $\Omega_m = 0.26$, that well satisfies $\Omega_b = 0.04$. The preferred value of baryonic density is

$$\Omega_b h^2 = 0.02273 \pm 0.00062,$$

where $h = 0.719 \pm 0.027$, is Hubble constant with units of kilometer per second per mega parsec. This constant determines the estimated value for the rate of expansion of the universe after the primordial big bang.

But there is a short fall because primordial nucleosynthesis examination reveals that the total baryon budget, including the contribution from stars in galaxies, intracluster stars and intracluster medium answers for only 90% of the baryons [31]. Although there are no fascinating arguments about this baryonic discrepancy, but we can say that there might be some unseen baryonic matter that can be fitted in to cope with the related difference. This matter could be present in intergalactic medium inside the clusters of galaxies. Or it might also lie inside the so called MACHOs (Massive Astrophysical Compact Halo Objects) [32] which circumscribe most neutron stars, white dwarfs[6], brown dwarfs[7], condensed objects such as black holes or non-luminous objects like planets.

Ω_Λ The Cosmological Constant

The big bang theory predicts the expansion of the universe, however, a naive expectation would be that of an expansion decelerated due to gravitational effects. Whereas, it is now known that this expansion is accelerated over time despite the inward pull of gravity. The cosmological constant is a parameter in General Relativity and as mentioned before, it can be defined as the energy of the vacuum of space. We can now write the total relic abundance (relativistic contribution not considered yet) of the universe as:

$$\Omega \equiv \Omega_m + \Omega_\Lambda,$$

where we have mentioned earlier $\Omega = 1$, obtained from the CMB results, we can write safely,

$$\Omega_\Lambda = 1 - \Omega_m.$$

Incorporating the value of Ω_m, we can see that Ω_Λ comes out to be 0.69 (1-0.31).

Relativistic Contribution to DM

[6]White dwarf is the last stage of the life of a star that has mass of the order of solar mass, and is reduced to the size of the Earth.

[7]Brown dwarfs are gaseous objects which are formed by the collapse of gas clouds but they have a very small mass and cannot form enough dense core to initiate hydrogen burning.

There is another contribution to the non-baryonic DM, which is due to the relativistic particles Ω_{rel}, but is almost negligible. These relativistic particles account for the electromagnetic energy and neutrinos. There are a number of experiments performed to determine the mass of the neutrinos present in the SM of particle physics. The density parameter for the neutrinos, lying in the mass range 5×10^{-4} to 1 MeV, is predicted to be [33],

$$\Omega_\nu h^2 = \frac{\sum m_\nu}{93eV}.$$

The most updated constraint from Planck measurement on the sum of neutrino masses is $\sum m_\nu < 0.68$ eV and the contribution of neutrinos to the DM relic density is given by [5]:

$$\Omega_\nu h^2 \leq 0.0025.$$

The amount of matter budget of the universe built from cosmological parameters, photons and neutrinos, is measured by CMB anisotropies with the help of Planck and WMAP satellites and the red-shift surveys of far away galaxies. The inhomogeneities and nature of perturbations in the universe through the matter and radiation spectra are also described to probe further [33].

The homogeneous universe's present-era state can be explained by writing the current-era values of all the density parameters. A typical collection, thus now, would include baryons Ω_b, cold DM Ω_{cdm}, photons and neutrinos Ω_{rel}. We can now write the total relic abundance of the universe as:

$$\Omega \equiv \Omega_m + \Omega_{rel} + \Omega_\Lambda.$$

The matter abundance, Ω_m, relativistic abundance, Ω_{rel} and the energy abundance, Ω_Λ in the universe are summarized here:

$$\Omega_m = 0.308 \pm 0.012, \text{ [33]}$$

$$\Omega_{rel} = 8.24 \times 10^{-5}, \text{ [26]}$$

$$\Omega_\Lambda = 0.692 \pm 0.012. \text{ [33]}$$

2.2.3 Existence

The evidences of existence of dark matter are confirmed on different scales and hence it can be said that dark matter can be made up of different substances which may not be the same for dwarf spirals and the Milky Way. A complete description on early history of DM with original references is given by S. Berg [34]. DM was first proposed in 1933 by Fritz Zwicky, who studied the coma cluster to account for the radial velocity dispersion of galaxies [35], that suggested the presence of non-luminous matter. He determined the relative velocities of the galaxies from their Doppler Shift for this system. From this, he quantified the mass that should provide the gravitational potential with which these galaxies should move. But this calculated mass was enormous, about 400 times greater than the observed stars confirming that there is large amount of matter which is not visible. In 1954, Martin Schwarzschild measured the mass-to-light ratio for different galaxies [36]. He obtained very high ratios which caused more confusion regarding the unseen matter. In August 1961, there held a conference in Santa Barbara on the subject of instability of galaxy systems. At the end of this conference, there was still no consensus on the dark matter hypothesis, however, the theory was not disregarded either. In fact there was an agreement upon collecting more information on the systems. In 1973, the work of Ostriker and Peebles was a turning point, which stated that instabilities in the galaxy disks models could be solved by the inclusion of massive hypothetical component known as DM **halo** [37]. A halo is considered to be the covering of galactic disc that extends beyond the end of visible galaxy. Ostriker and Peebles along with Yahil, also noted that the galaxy masses keep on increasing with radius [38]. These results, together with recent velocity curves, provide overwhelming evidence for the 'missing mass' in galaxies.

The rotation curve or the velocity curve of any galaxy exhibits a plot of the orbital speed of the stars versus their radial distances from the centre of the galaxy. For a galaxy it is observed that most of the stars reside at it's center, where they are visible, so the major proportion of visible mass of galaxy is concentrated at the center. According to Newton's law of gravitation and dynamics, if we move away from this mass distribution, then these velocities should drop as $1/\sqrt{r}$, where r is

the distance from the center of the galaxy. But the velocities remain constant, or flat, for almost all cases, after a rise from r = 0 and upto very large radii, that essentially included all of the galaxy's light. Thus, we cannot say how far from the center of galaxy, the dark halos are extended. The following Fig. 2.2 shows the rotation curve for the spiral galaxy NGC 6503 [35],[39]. Here it was expected

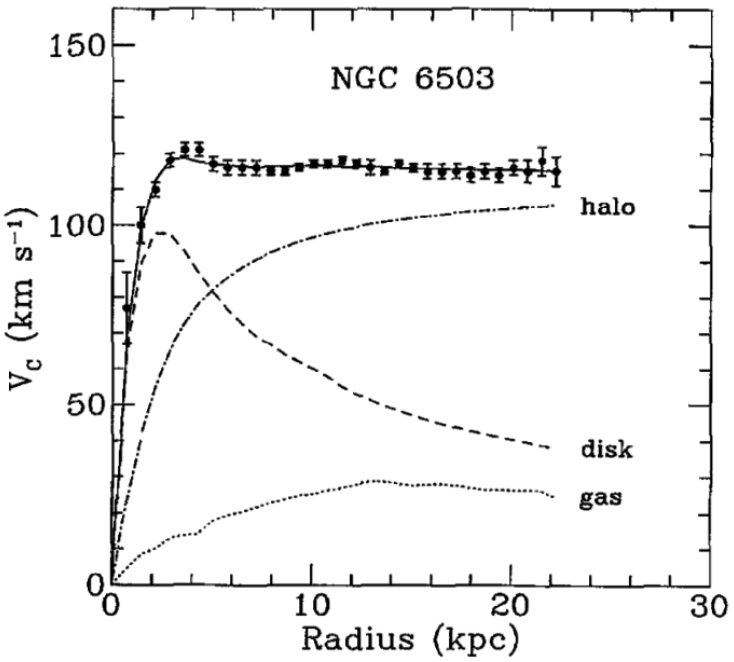

Figure 2.2: Rotation curve of NGC 6503. The dotted, dashed and dashdotted lines are the contributions due to gas, galactic disk and dark matter halo, respectively. From Ref. [45].

that the rotation curve would have dropped at large radii if only luminous matter was there. The measured rotation curve is observed to be remain flat from about 4 kpc to about 18 kpc. Thus, the existence of a dark matter halo is confirmed by the discrepancy between the rotation curve for the luminous disk and gas and the observed rotation curve.

Several substantial reviews about the dark matter physics [13],[40],[41],[42] have been written, as well as many books [43],[19],[44] also exist to understand the chief candidates of DM. In this thesis the focus is maintained on the prime candidate, lightest supersymmetric particle, which belongs to the class of weakly interacting

massive particles (WIMPs). It has become a guide for DM and is the lightest of all the hypothetical particles in the supersymmetric theory beyond the SM, which is discussed in next chapter.

2.2.4 WIMP as DM Candidate

The most important and largest class of non-baryonic cold dark matter candidate includes Weakly Interacting Massive Particles (WIMPs), that were created thermally at an early time of the universe. Using the WIMP scenario, density of dark matter in this universe could be build up.

In the standard WIMP scenario, it is considered that WIMPs were produced, in the early universe, when particles of thermal plasma collided with each other. The important reaction, in this radiation-dominated era,included the creation and annihilation of WIMP pairs during collisions of particle-antiparticle pairs. e.g.,

$$\chi\bar{\chi} \leftrightarrow q\bar{q}, \mu^+\mu^-, e^+e^-, W^+W^-, HH, ZZ, ...$$

At this stage, the plasma's temperature was very much higher than the mass of the WIMP (T>> χ_m) and the particle-antiparticle pair collided with each other frequently to create pairs of WIMPs. The inverse reactions, at this stage, where WIMPs annihilated into standard model particles, were also in equilibrium with the production process of WIMP. The number density of the WIMP, at this stage, n_χ is proportional to T^3 i.e.,

$$n_\chi \propto T^3,$$

With the expansion of the universe, the temperature dropped below the mass of the WIMP (T<< χ_m), and at temperature less than the mass of the WIMP, the number of WIMPs which were being produced, decreased exponentially with time as shown in Fig. 2.3:

$$n_\chi \propto e^{-m_\chi/T}.$$

With the decrease in number density, the annihilation rate of WIMPs also decreased. As the annihilation rate of the WIMP became smaller than the Hubble's expansion rate of the universe or we can say that the mean free path of the reactions/collisions

producing WIMP becomes longer than the Hubble's radius, WIMP reach "freeze-out" or chemical decoupling and their number per comoving volume became constant over time, shown by the dashed black line.

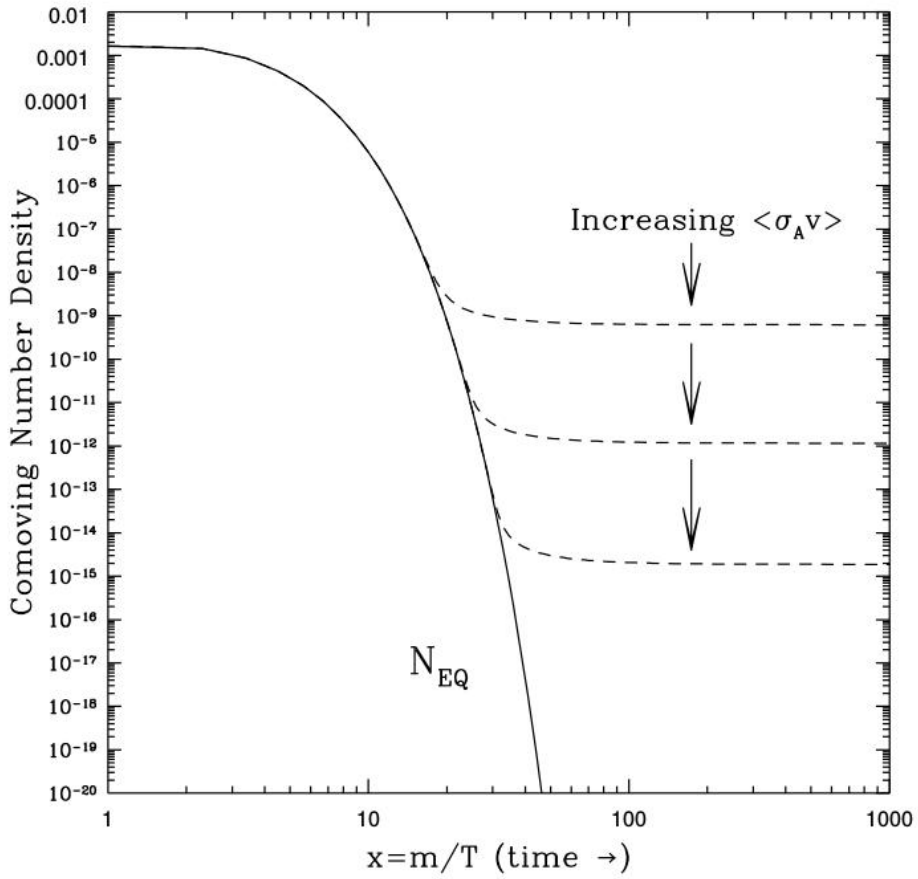

Figure 2.3: General evolution of WIMP number density in the early Universe. The dashed curves represent actual relic abundances for different cross sections, and the solid curve is the equilibrium abundance [13].

Cosmological WIMP abundance Ω_χ is given by an approximate solution to the Boltzman equation,

$$\Omega_\chi h^2 = m_\chi n_\chi / \rho_c \cong 0.1(3 \times 10^{-26} cm^3 sec^{-1}) / < \sigma_A v > . \qquad (2.1)$$

If the annihilation cross section, $< \sigma_A v >$, according to this equation is roughly the

order of

$$3 \times 10^{-26} cm^3 sec^{-1} (10^{-8} GeV^{-2}), \tag{2.2}$$

then WIMP relic density comes out to be about 0.1. Interestingly, the cross section for electroweak interactions is also of this magnitude, i.e.,

$$\sigma_{weak} \cong \alpha^2 / m^2{}_{weak}, \tag{2.3}$$

where α is related to electroweak coupling and is of the order of 0.01, whereas, m_{weak} is of the order of 100 Gev. This gives the same number as in Eq. (2.1). This coincidence implies that, if there exists a massive particle that is stable and interacts through electroweak interactions, then it is accountable for dark matter candidate. This is also known as WIMP miracle. So if we build an accelerator that can provide collisions for elementary particles at energies higher than 100 Gev, then we might be able to produce WIMPs that have mass around 100 Gev.

Finally, there might be a likelihood of other possibilities, that are not adjusted easily into the above classification scheme. Also, they do not have that strong theoretical arguments as those of WIMPs, but they do lie in the domain of possibility.

Neutralinos

Neutralino is one of the most studied candidate of DM belonging to the class of WIMPs. As explained in the first chapter, neutralino is the super-partner of more than one particle in SM. It is a linear combination of Z-ino, higgsino and photino (superpartners of Higgs boson, the neutral Z boson and photon respectively). There are various arguments for declaring neutralino as a favorable candidate for DM in the theory. They possess considerable amount of mass needed to account for the DM relic density of the universe, and thus are able to produce enough gravitational influence to their neighbors. The theory also predicts that these neutralinos are produced in abundant quantity as those of protons and neutrons. The more details about this candidate are given in next chapter.

2.2.5 Direct and Indirect Detection

Dark Matter particles as WIMPs interact gravitationally and their interactions are very weak such that they will make their way by the earth unnoticeable. Few of the energetic WIMPs will transfer their kinetic energy partially to the terrestrial nuclei on collision. Direct detection processes involve the method of observing that how much energy is deposited to the recoiled nuclei. For this, very large detectors are built to observe the events with larger effective area.

For detecting DM through direct detection, detectors containing large quantity of some element is built and it detects small interactions between atoms within this detector. If DM particles exist everywhere through and around the earth, then they are available in detectors as well. It is possible that DM particle might enter the detector and interacting through weak interactions, it deposit some energy to the nucleus of the atom in a detector. The experiments of direct detection detect the WIMPs through nuclear recoils during the WIMP-nucleus elastic scattering. In particular, the experiments tend to find the rate R and recoiled energy, E of nucleus.

The differential rate of scattering for WIMP and nuclei expressed usually in terms of counts per Kg per day per kilo electron volt (unit of differential rate or dru), is given as,

$$\frac{dR}{dE}(E,t) = N_T \frac{\rho_\chi}{m_\chi} \int_{v_{min}} \frac{d\sigma}{dE}(v,E) v f(v) d^3v, \tag{2.4}$$

where the number of targeted nuclei is denoted by N_T, ρ_χ is the number density of WIMPs, m_χ is their mass and v is their velocity relative to the earth. $\frac{d\sigma}{dE}(v,E)$ is WIMP-nucleus differential cross-section for the scattering of nucleus and incoming DM particle. $f(v)$ is the speed distribution of WIMP, which accounts for the probability of finding any DM particle moving with the velocity v at any time t.

The recoiled energy of the nucleus can easily be calculated, in the centre of mass frame, in terms of scattering angle θ:

$$E = \frac{\mu^2 v^2 (1 - cos\theta)}{m_N}$$

where $\mu = \frac{m_\chi m_N}{(m_\chi + m_N)}$ is the reduced mass of WIMP and nucleus.

The lower limit of integration is given by, $v_{min} = \sqrt{m_N E/2\mu^2}$, which is the minimum velocity of the DM particle, required to produce a recoil in order to deposit considerable amount of energy in the detector [46]. While the upper limit is formally infinite.

DM particle or WIMP may go through interaction with detector material and this interaction can be elastic or inelastic, also the process can be spin-dependent or spin-independent. An elastic scattering will result in a collision of DM particle with a nucleus as a whole that causes the nucleus to recoil and hence is the reason of depositing energy in the detector. Whereas, in an inelastic scattering the advancing DM particle can cause the target particle to go into some higher excited state rather than only producing a recoil in it. Later it is decayed by emitting photons. Spin-dependent interaction would be the one where spin of DM particle is coupled with that of target material, whereas, this does not happen in spin-independent interaction. In short we can say that if a signal is detected in a detector, then by relating the mass and scattering cross section of the DM particle to it's local density, we can infer the existence of DM particle.

The DM particles can also be detected indirectly as they annihilate into product particles. Neutralinos, e.g., in SUSY, are majorana particles that annihilate with each other. Thus by self-annihilating they may yield a flux in the background, composed of neutrinos, cosmic rays and gamma rays which might appear as an excess in the background as expected. Due to the annihilation of these DM particles, the emerging flux can be written as:

$$\frac{d\Phi}{d\Omega dE} = \frac{\sigma v}{8\pi m_\chi^2} \times \frac{dN}{dE} \times \int_{L.O.S} ds\ \rho^2(r(s,\Omega)). \tag{2.5}$$

Here σv is annihilation cross section, Ω is the solid angle of the concerning area, $\rho(r(s,\Omega))$ is the local DM density, dN/dE determines the energy spectrum which, in case of gamma rays, would account for the number of photons per annihilation. We can see that flux of the DM particle produced, is directly proportional to the square of it's density, hence indirect detection is more sensitive to cosmological effects than direct detection. Results of capturing some DM particles through indirect detection may vary as a result of annihilation products e.g., gamma rays, neutrinos, anti-matter e.t.c. Some detectors might get a track of dark matter through the

emergence of high energy cosmic ray positron signal [47] whereas high energy neutrino telescopes could also be used for detecting dark matter [48],[49]. The idea is to think WIMPs residing in some more massive object like sun, where they annihilate with each other at high rates, and producing significant amount of neutrinos, which can be detected in a detector.

For the direct detection of DM particles or WIMPs, the current searches are active through large underground Xenon (LUX) experiment. Xenon DM search program includes Xenon10 (2007), Xenon100 (2016) and Xenon1T (2017) [50]. The Xenon1T experiment uses 3.2 tons of liquid Xenon in a time-projection chamber to identify the weakly interacting DM particles interactions individually. The principle is based on the isolation of detector by surrounding water tank from earth and background particles. This shielding minimizes the interaction of cosmic rays and radiations with Xenon.

Another series of experiments leading the direct detection field, is cryogenic dark matter search (CDMS). The CDMS experiment started in 2002 in Minnesota. The scientists renamed it as SuperCDMS (SCDMS) after installing advanced Germanium detectors in 2010. The SCDMS experiment aims at measuring the recoil energy transferred to Germanium nuclei during nucleon-WIMP collision. The outfitted sensors detect the ionization and phonon signals in the background [51].

For indirect detection of WIMPs, the IceCube neutrino observatory is constructed at earth's South Pole which detects the neutrino signals from the self annihilation of WIMPs in the galactic halo and the galactic center.

It's principle is based on the fact, that if we have some source of neutrinos, we may calculate the amount of neutrinos that it is emitting and also the amount that it must produce. However, if the difference between the two is greater than zero then it might account for missing DM relic density. When the cosmic neutrinos reach the ice, it may interact weakly with the ice's nucleons through inelastic scattering. The decaying products then emit Cherenkov radiation as they travel through the ice and hence detected by the Digital Optical Modules (DOMs) to record the neutrino signal.

There are other experiments, Fermi LAT (**F**ermi **L**arge **A**rea **T**elescope) and PAMELA (**P**ayload for **A**ntimatter **M**atter **E**xploration and **L**ight-nuclei **A**strophysics),

which search for the existence of DM particles when WIMP annihilates into matter-antimatter and gamma radiations respectively.

Chapter 3

Minimal Supersymmetric Standard Model

3.1 Supersymmetry

The nature of dark matter is somehow accommodated by the realm of supersymmetry. Supersymmetry (SUSY) is a purely hypothetical symmetry generated by theory. It is a very refined and sophisticated extension of the SM, and is the generalization of the space-time symmetries of the quantum field theory, in which we relate the fermionic degrees of freedom to the bosonic one.

For understanding, let us consider a continuous symmetry of space translations and rotations. A 3-dimensional rotation is described completely by three parameters i.e., 3 angles denoted by Θ and the translational parameter is denoted by $\vec{a}$. Then under this transformation;

$$\vec{x} \rightarrow \vec{x'} = R(\vec{\Theta}).\vec{x} + \vec{a}. \tag{3.1}$$

R is a 3×3 rotation matrix which depends on Θ.

However, if we expand the symmetry group to include the Poincare group consisting of Lorentz transformations and translations, then we can write:

$$x^{\mu} \rightarrow x'^{\mu} = x^{\mu} + \Lambda^{\mu}{}_{\nu}\, x^{\nu} + a^{\mu}, \tag{3.2}$$

where $x^{\mu} = (t, \vec{x})$ represents the coordinates in Minkowski space-time.

In Eq. (3.2), the symmetry group has now been increased to 10 generators as compared to Eq. (3.1) which has only 6 generators including 3 for rotations and 3 for translation. However, in Eq. (3.2), there are 6 Lorentz transformation parameters and 4 translation parameters a^μ. 6 Lorentz transformation parameters contain three rotation angles and three boost parameters, which are written in terms of an antisymmetric tensor,

$$J^{\rho\sigma} = -J^{\sigma\rho},$$

where $\rho \in (1, 2, 3, 4)$ and $\sigma \in (1, 2, 3, 4)$ are Lorentz labels. The four generators of translations are represented by P^ρ. The two quantities P^ρ and $J^{\rho\sigma}$ correspond to the four-momentum and the generalized angular momentum. Now the commutation relations, known as the algebra of Poincare group, can be written for various P^ρ and $J^{\rho\sigma}$:

$$\begin{aligned}
&[P^\rho, P^\sigma] = 0. \\
&[P^\rho, J^{\nu\sigma}] = i(g^{\rho\nu}P^\sigma - g^{\rho\sigma}P^\nu). \\
&[J^{\mu\nu}, J^{\rho\sigma}] = -i(g^{\mu\rho}J^{\nu\sigma} + g^{\nu\sigma}J^{\mu\rho} - g^{\mu\sigma}J^{\nu\rho} - g^{\nu\rho}J^{\mu\sigma}).
\end{aligned} \tag{3.3}$$

In gauge theories, we can always extend the Poincare symmetry further. Consider a gauge group SU(N), for which we keep on adding generators, T^a with $a \in (1, 2, ..., N^2 - 1)$, having $N^2 - 1$ parameters. This kind of extension is known as 'trivial' because now all the new generators commute with the old ones.

$$\begin{aligned}
&[T^a, T^b] = if^{abc}T^c. \\
&[T^a, P^\rho] = 0. \\
&[T^a, J^{\rho\sigma}] = 0.
\end{aligned} \tag{3.4}$$

where f_{abc} are structure constants. This means that the extended symmetry group is a direct product of the Poincare group with a gauge (or internal symmetry) group.

The extensions of this type of Poincare group are significant and very successful in describing particle interactions. But what if we extend the group in non-trivial way, so that the new generators also mix with P^ρ and/or $J^{\rho\sigma}$. Coleman-Mandula no-go theorem is considered as a central idea in this regard. This theorem says that the internal symmetry and the space-time symmetry cannot be combined except

the trivial way. While proving the Coleman-Mandula theorem, it was implied to use only bosonic generators. Here it is important to note that a generator that converts one bosonic state to another, or one fermionic state to another fermionic state, is known as bosonic generator. All the generators P^{ρ}, $S^{\rho\sigma}$ and G^{a} are bosonic generators because spin of the state, to which they act upon, does not change. Now the fermionic generators, i.e., the generators that change the spin of the state upon which they act on, are also allowed in the algebra. As it acts on a scalar state having spin 0, it will generate a state having spin 1/2. If the fermionic generator is denoted by Q_{α}, we can write,

$$Q_{\alpha} \ |bosonic\ state\rangle \ = \ |fermionic\ state\rangle_{\alpha} \, ,$$

$$Q_{\alpha} \ |fermionic\ state\rangle^{\alpha} \ = \ |bosonic\ state\rangle \, .$$

Hence we can see that the fermionic partners in SM with spin half, have bosonic partners in SUSY with spin 0, but otherwise have the same quantum numbers corresponding to internal symmetries. SUSY transformations, that convert a boson into a fermion and vice-versa, leave the Lagrangian invariant. The supersymmetric particles which are the super partners of SM fermions are designated with an additional s and designated by an overhead $\sim$, for example, the super partner of top is named as *stop* represented by $\tilde{t}$. And all the super partners of SM bosons have an *ino* at the end, for example, bino, wino, Higgsino, photino e.t.c.

If SUSY exist at all, it must be a broken symmetry. Because if it were an exact symmetry, the SUSY particles would have same mass as those of SM particles. Since we know experimentally, that there are no SUSY particles seen at this energy scale, so it must be a broken symmetry. SUSY ultimately also solves the Gauge hierarchy problem which attributes to the large hierarchy of the energy scales of M_z and Planck. The supersymmetric generalization of SM can be established using the standard concepts of QFT, that can be checked experimentally, leading us to the Minimal Supersymmetric Standard Model (MSSM), discussed next.

3.2 Minimal Supersymmetric Standard Model

3.2.1 The structure of the MSSM

The word *minimal* refers to the choice of taking minimum particle spectrum to get the model work. The SM is made supersymmetric in a minimal way by adding the supersymmetric partners of the SM and incorporating, the two Higgs-doublet. The reason for including two Higgs doublet is that, it cannot contain the adjoint of superfields because it is technically not allowed. So the masses cannot be given to both of up-type and the down-type quarks by the same Higgs multiplet. Thus, two Higgs fields are required, one with hypercharge $Y = 1/2$, and other with $Y = -1/2$, for all types of quarks.

The Lagrangian is obviously constructed to be invariant under $SU(3)_c \times SU(2)_L \times U(1)_Y$ as well as superspace translations, and is invariant not only under the SM gauge group (described in section 2.1) but is also invariant supersymmetrically. Quantum fields in supersymmetric theories are known as superfields. The SM gauge fields are part of Vector superfields and matter fields are part of chiral superfield. So the fermions whose left-handed components are transformed differently from those of right-handed, are contained in different chiral supermultiplets. The scalar partners interact through the same gauge interaction as the corresponding SM fermions. The basic structure of all the particles is given in Table 3.1.

In the first, second and third column, are the superfields, bosonic component and the fermionic component respectively. Row wise, the table is distributed in three partitions. Gauge-supermultiplet (particle along with it's superpartner form a supermultiplet), contain the gauge fields G^a related to $SU(3)_c$, V^k related to $SU(2)_L$, and last is V' related to $U(1)_Y$. G^a contains the SM gluons and their superpartners, the gluinos. V^k contains the SM weak bosons and their superpartners winos. Finally, V' contain the hypercharge B and it's supersymmetric partner bino.

In the second partition, the chiral superfields are placed. L_i, E_i, Q_i, U_i, D_i are the fields which have been described in Table 2.1, while the bosonic column contains the Sleptons and squarks. Here it should be known that the supersymmetric partner of the right-handed component of electron (muon, tau) is named as selectron (smuon,

Table 3.1: The Particle spectrum in MSSM.

Superfield	**Bosons**		**Fermions**	
Gauge				
G^a	gluon	g^a	gluino	$\tilde{g}^a$
V^k	Weak	W^k	wino	$\tilde{w}^k$
V'	Hypercharge	B	bino	$\tilde{b}$
Matter				
L_i	Sleptons	$\tilde{L}_i = (\tilde{\nu}, \tilde{e})_L$	Leptons	$L_i = (\nu, e)_L$
E_i		$\tilde{E}_i = \tilde{e}_R$		$E_i = e_R$
Q_i	Squarks	$\tilde{Q}_i = (\tilde{u}, \tilde{d})_L$	Quarks	$Q_i = (u, d)_L$
U_i		$\tilde{U}_i = \tilde{u}_R$		$U_i = u_R$
D_i		$\tilde{D}_i = \tilde{d}_R$		$D_i = d_R$
Higgs				
H_u	Higgses	H_u	Higgses	$\tilde{H}_u$
H_d		H_d		$\tilde{H}_d$

stau). Also the SUSY partners of neutrinos are called as sneutrinos, whereas for the quarks, the SUSY partner of up (top, bottom, e.t.c) is sup (stop, sbottom, e.t.c).

Lastly, the Higgs sector contains two Higgs supermultiplets coupling to the up-type and down-type superfields. The SUSY partners of the Higgs field are named as higgsinos.

3.2.2 The superpotential of the MSSM

The SM contains all the allowed renormalizable interactions, permitted by its gauge group, whereas the superpotential written for MSSM contains only the interactions which are required to be consistent with SM. The terms which are gauge invariant and also respect the Baryon and Lepton number invariance are added in the MSSM.

The superpotential of MSSM is written as,

$$W_{MSSM} \;=\; y_u^{ij} Q_j U_i H_u \;-\; y_d^{ij} Q_j D_i H_d \;-\; y_e^{ij} L_i E_i H_d \;+\; W_\mu, \tag{3.5}$$

where $W_\mu = \mu H_u H_d$.

$y^{ij}s$ are the 3×3 Yukawa coupling matrices in family space, and μ is bilinear Higgs mixing mass parameter in SUSY. The fields that are appearing here, are the chiral fields defined in Table 3.1. Family and gauge indices have been suppressed while writing this superpotential. The μ term is the supersymmetric version of the SM Higgs mass term. It is worth noting at this point that in MSSM we have more interactions available than in the SM, like y_u, y_d, y_e are now also responsible for squark-Higgsino-quark and slepton-Higgsino-lepton interactions. $\mu H_u H_d$ is a bilinear mixing term, which is added to avoid massless Higgs state.

The MSSM model is limited and include the only interactions that are required by the SM and it's supersymmetric generalization. In spite of superpotential terms in Eq. (3.5), there are several other terms that are consistent with the internal symmetries of the theory. e.g., the terms that could be added are:

$$W_R = \frac{1}{2}\lambda L_i L_j e_c + \lambda' L_i Q_i d_c + \frac{1}{2}\lambda'' u_c d_c d_c + \mu' L_i H_i \tag{3.6}$$

All of these terms are R-parity [52] violating terms, suppressed with one or more generation indices in each term. R is defined as $R = (-1)^{3(B-L)+2S}$ for a particle of spin S. Here it can be noted easily that the terms which are proportional to λ, λ' and μ', all violate the lepton number by one unit. Whereas, the term which is proportional to λ'' violates the baryon number by one unit. In Eq. (3.6) we can see that if λ' and λ'' are non-zero, it will lead to rapid proton decay processes through, $p \to \nu\pi^+$, νK^+, $e^+\pi^0$, $\mu^+\pi^0$, e.t.c.

All the SM particles have even R-parity while their SUSY partners have odd parity. By imposing this R-parity in decay and scattering processes, we can see that the problem of rapid proton decay and the lightest supersymmetric particle (LSP) is also stable as an aftermath of R-parity invariance, which must be produced at the end of decay chain of heavy supersymmetric particles.

3.2.3 The SUSY Lagrangian

In order that MSSM couple to gravity, a graviton super-multiplet is introduced. This super-multiplet contains spin-3/2 gravitino and spin-2 graviton. It is not necessary that they are connected minimally to the MSSM. For the gravity to be consistent at the quantum level, it requires that the SUSY be broken spontaneously [53],[54]. However, the mechanism of SUSY breaking is unknown. Whereas to retain the large hierarchy between the Planck and electroweak scale, it is required that this symmetry should be broken 'softly' so that the quadratic divergences remain out of the theory.

By considering all the supersymmetric interactions, the Lagrangian of MSSM is established that must satisfy the gauge invariance of $SU(3) \times SU(2) \times U(1)$, and the conservation of Baryon and Lepton number as global symmetries. Those terms are added in the SUSY Lagrangian because of which SUSY is broken explicitly. These terms are called soft supersymmetry breaking (SSB) terms and the coefficients that appear with these SSB terms are known as SSB parameters.

Following set of parameters are included in supersymmetric breaking sector:

M_1, M_2 *and* M_3 are the gaugino masses associated with the SM subgroups, U(1), SU(2) and SU(3) respectively.

Corresponding to sfermions, there are five squared mass parameters, $M^2_{\tilde{E}}, M^2_{\tilde{L}}, M^2_{\tilde{U}}$, $M^2_{\tilde{D}}, M^2_{\tilde{Q}}$, which are scalars.

The trilinear interaction terms, Higgs-slepton-slepton and Higgs-squark-squark, include A_U, A_D, and A_E and are known as A-parameters.

SUSY Lagrangian for MSSM can be written as,

$$\mathcal{L} = \mathcal{L}_{SUSY} + \mathcal{L}_{soft}$$

part of the Lagrangian, $\mathcal{L}_{soft}$, contains all the SSB terms,

$$\begin{aligned}\mathcal{L}_{soft} = -\frac{1}{2}\left(M_1\tilde{b}\tilde{b} \;+\; M_2\tilde{w}\tilde{w} \;+\; M_3\tilde{g}\tilde{g}\right) \;+\; h.c. \;-\; m^2_{H_u}h^\dagger_u h_u \;-\; m^2_{H_d}h^\dagger_d h_d \\ -\left(bh_u h_d + h.c.\right) - \left(A_u\tilde{u}_R\tilde{q}h_u \;+\; A_d\tilde{d}_R\tilde{q}h_d \;+\; A_e\tilde{e}_R\tilde{L}h_u\right) \;+\; h.c. - \; m^2_Q\tilde{q}^\dagger\tilde{q} \\ - \; m^2_L\tilde{l}^\dagger\tilde{l} \;-\; m^2_u\tilde{u}^\dagger_R \;-\; m^2_d\tilde{d}^\dagger_R\tilde{d}_R \;-\; m^2_e\tilde{e}^\dagger_R\tilde{e}_R. \qquad (6)\end{aligned}$$

Definitions of all the fields are defined distinctly in the table 3.1, whereas, the A-parameters and the squared masses, $m^2_{\tilde{E}}, m^2_{\tilde{L}}, m^2_{\tilde{U}}, m^2_{\tilde{D}}, and m^2_{\tilde{Q}}$ are the matrices of the order 3×3 in generation space. All the terms included in the Lagrangian are of positive mass dimension or of zero mass dimension.

3.2.4 The neutralino mass eigen-state

The gluinos are degenerate in mass in terms of mass eigenstates, while the charged winos along with the charged higgsinos mix to give up two charginos. They are denoted as $\tilde{\chi}^{\pm}_{1,2}$. And the neutral wino, bino and the neutral higgsinos combine to give, the four neutralinos, denoted as $\tilde{\chi}^0_{1,2,3,4}$. Among these, the lightest neutralino, $\tilde{\chi}^0_1$, being electrically neutral and colorless, is of extensive importance. In MSSM, lightest neutralino, known as lightest supersymmetric particle (LSP) is an excellent candidate for DM.

The mass of LSP and it's physical state, and the ratio of it's mixing components can be found by diagonalizing the following mass matrix:

$$M = \begin{bmatrix} M_1 & 0 & -m_Z sin\theta_W cos\beta & -m_Z sin\theta_W sin\beta \\ 0 & M_2 & m_Z cos\theta_W cos\beta & -m_Z cos\theta_W sin\beta \\ -m_Z sin\theta_W cos\beta & m_Z cos\theta_W cos\beta & 0 & -\mu \\ m_Z sin\theta_W sin\beta & -m_Z cos\theta_W sin\beta & -\mu & 0 \end{bmatrix}$$

This matrix is written in the basis of $\tilde{W}, \tilde{B}$ and Higgsinos, $\tilde{H_1}$ and $\tilde{H_2}$. M_1, M_2 and μ are the mass parameters of bino, wino and higgsino respectively, while θ_W is the weak angle. The LSP is the lightest eigenvalue derived from this matrix and its nature depends on relative magnitudes of δ, γ, β and α. The constituents of lightest neutralino can be written as,

$$\chi^0_1 = \delta\tilde{B} + \gamma\tilde{W} + \beta\tilde{H_1} + \alpha\tilde{H_2},$$

Normalizing this equation gives unity:

$$\delta^2 + \gamma^2 + \beta^2 + \alpha^2 = 1$$

$|\delta|^2$ represents the probability of the neutralino being a bino, $|\gamma|^2$ represents that of wino and so on. Thus if we say that the bino content of the LSP is maximum, then we mean that $\delta^2 \simeq 1$, or if the wino content is maximum then $\gamma^2 \simeq 1$ and so on.

In SUSY we know that there exist scalar partner allies for the known fermions, while for the known vector bosons, there are new fermions. But experimentally, it is not justified unfortunately. Likewise, in the SM, the massive vector bosons should remain massless, but by introducing the Higgs mechanism and spontaneous symmetry breaking in the scalar potential [1], this problem can be solved. By breaking the symmetry of the vacuum state, and keeping the Lagrangian gauge symmetric, the vacuum supplies the masses to the apparent massless bosons. Hence, by spontaneous symmetry breaking, we can break the supersymmetry such that it is possible to generate all the masses of the supersymmetric particles.

[1]The potential of the Lagrangian are those terms not containing derivatives of the fields (kinetic terms). And the scalar potential are such terms that contain only scalar fields.

Chapter 4

Dark Matter Scenarios In constrained minimal supersymmetric standard model

4.1 Constrained minimal supersymmetric standard model (cMSSM)

The Constrained Minimal Supersymmetric Standard Model (cMSSM) [70],[71],[72],[73],[74],[75] incorporates universal boundary conditions at the GUT scale for the soft SSB terms. The parameters of this model are,

- universal scalar mass of the sfermions, m_0.
- universal gaugino mass, $m_{1/2}$.
- the universal trilinear coupling, A_o.
- the ratio of the up and down Higgs vacuum expectation values (VEVs), $tan\beta = \frac{<H_u>}{<H_d>}$.
- the sign of μ.

where μ is the Higgs mass mixing parameter, that mixes the superfields, H_1 (related to up-type quark) and H_2 (related to down-type quark).

Thus cMSSM is parametrized in such a way that it has just five more additional parameters than SM, and it is able to generate the mass spectrum for all the su-

persymmetric partners of SM. All the SSB parameters are evolved from M_{GUT} to M_{Weak} through their RGEs. At M_{weak}, the electroweak gauge symmetry is broken radiatively. We incorporate the $SOFTSUSY-4.0$ [76] RGE code for this model to calculate the energy spectrum of all the sparticles. Then MSSM package within $MicrOMEGAs-4.2.5$ [77] is interfaced with $SOFTSUSY$ to generate the results for neutralino DM density.

4.2 Annihilations and Coannihilations

Annihilations take place through virtual particles, which are basically short-lived and transient. According to Heisenberg's uncertainty principal, if these virtual particles come into existence for extra ordinary short time, then there is no overall violation in the laws of Physics.

In an annihilation process, a particle and an anti-particle annihilate together completely into energy. They interact in such a way that their energy is converted into force carrier-particles like gluons, photons and W or Z-bosons, and then undergo different transformations and are converted to some low-mass particles.

It was discussed in chapter 2, that in the early era of universe, the DM particles kept on annihilating into SM particles and so on. For greater annihilation rate, they could annihilate for longer time and it will correspond to less DM relic density. However, for smaller annihilation cross section rate, they would have come out of equilibrium too quickly and DM relic density will be greater, which is also clear from Eq. (2.1). In our model, i.e., constrained minimal supersymmetric model, we come across different annihilation channels for which value of relic density is decreased to zero almost. In the Fig. (4.1), we can see that the value of relic density goes to zero through light Higgs pole annihilation channel, $\chi\chi \to h$. We can see that the value of relic density goes to zero when the mass of two neutralinos becomes equal to Higgs mass m_h.

Since the amplitude $\approx 1/(p^2 - m^2)$, where p is the momentum of h/Z, therefore two annihilating particles that annihilate at zero speed, their momentum is equal to their mass and thus we get a zero in the denominator. Because of this we see a blow up in the cross-section that is known as resonance. Near a pole, any function changes

rapidly and thus rapidly changing annihilation cross section produces rapidly varying values of relic density.

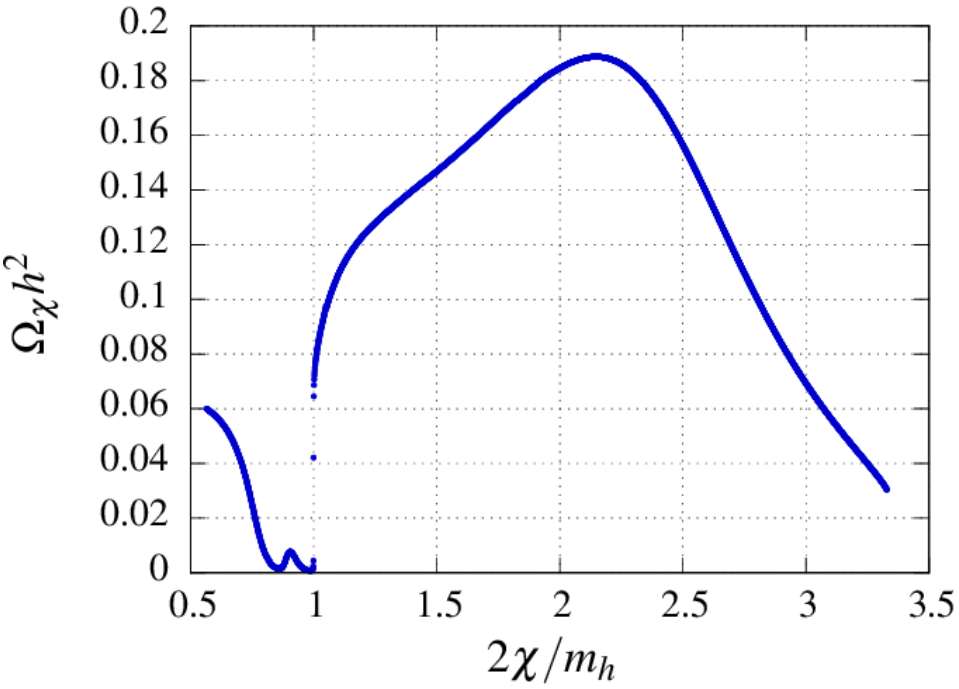

Figure 4.1: Light Higgs-resonance annihilation.

Similarly, in Fig.(4.2) and (4.3), Z-resonance annihilation and heavy neutral Higgs boson annihilation channels are shown respectively. On y-axis values of relic density $\Omega_\chi h^2$ are plotted while on x-axis the ratio of two neutralinos and m_Z for Fig. (4.2) and ratio of two neutralinos and m_A for Fig. (4.3) is plotted. It is obvious that the dip in relic density appears exactly where mass of two neutralinos becomes equal to m_Z or m_A.

Coannihilations refer to the annihilations of lightest supersymmetric particle (LSP) and next to lightest supersymmetric particle (NLSP). If any supersymmetric particle has roughly the same mass as that of DM candidate (neutralino in our case), then they coannihilate.

There are different scenarios, in which the mass of the LSP is comparable to any of the sparticles and hence the relic abundance of the LSPs is greatly affected by the co-annihilations. In ref [55], Griest and Seckel indicated the case where squarks have

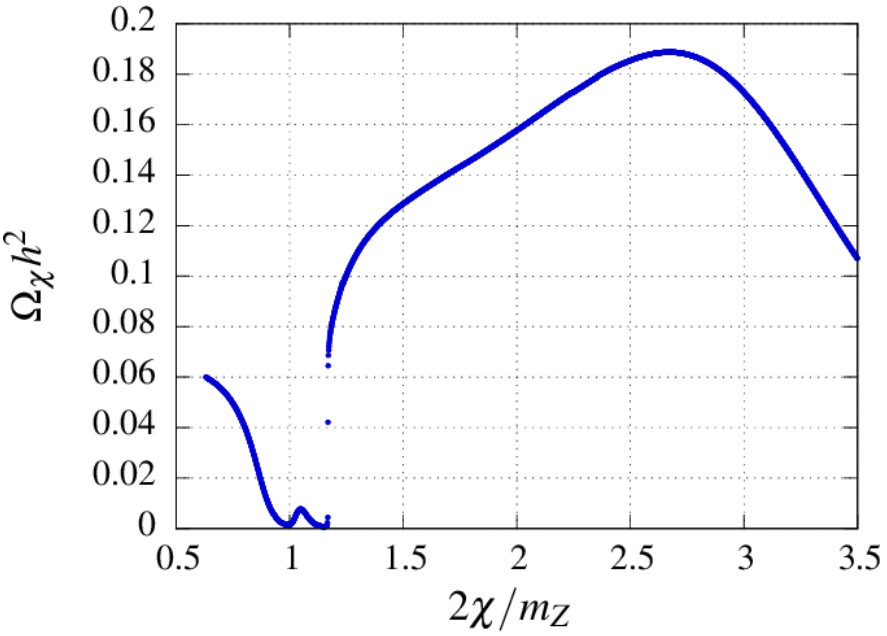

Figure 4.2: Z-resonance annihilation.

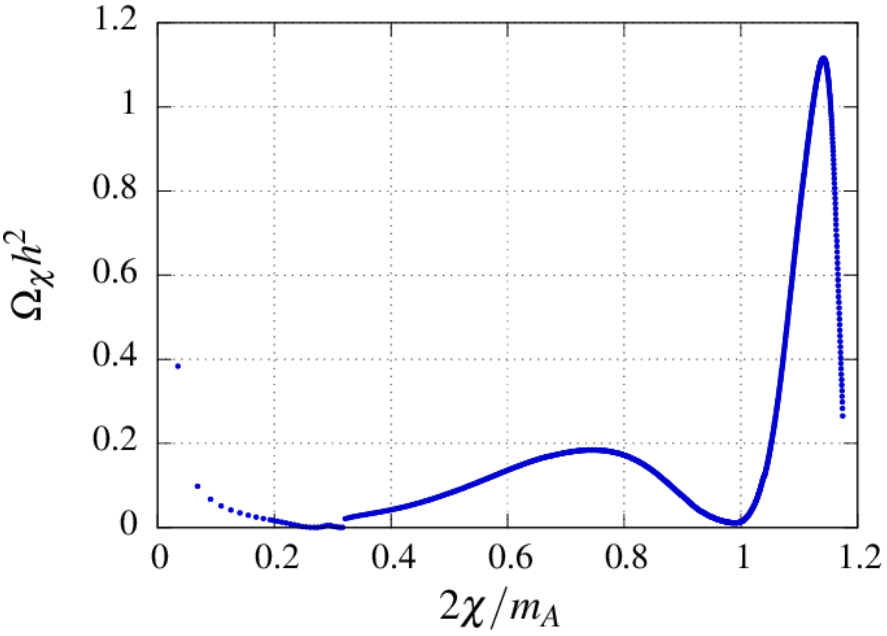

Figure 4.3: A-resonance annihilation.

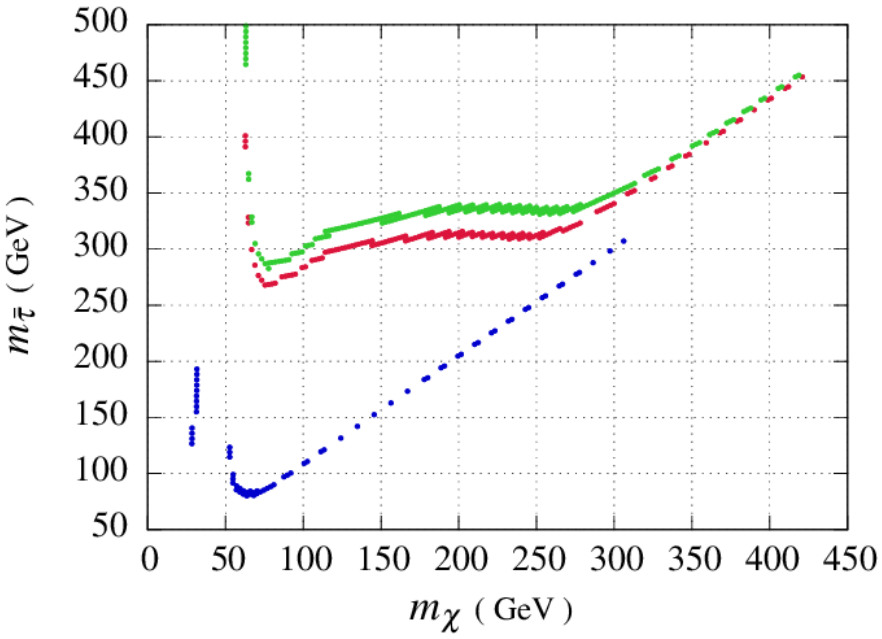

Figure 4.4: Plots of relic density in χ-$\bar{\tau}$ plane to show $\bar{\tau}$ and χ co-annihilation - Blue contour stands for $\Omega_{\chi}h^2$=0, red contour stands for $\Omega_{\chi}h^2$=0.1, and green contour stands for $\Omega_{\chi}h^2$=1,

their mass very close to the LSP, which causes the relic abundance to be lowered significantly due to the co-annihilations with squarks. Appropriate values of relic density are attained with the help of the co-annihilations with sleptons, such as stau $\tilde{\tau}$ that occurred in the regions where stau is nearly degenerate with neutralino χ, which brings the relic density to cosmologically acceptable values. The neutralino and slepton annihilation is enforced at several places [83],[56],[57],[58],[59]. The regions for low m_0, where neutralino is degenerate with stau, both for low and higher values of tanβ, the co-annihilations could provide with rational values of relic density, even when values of $m_{1/2}$ are large. The neutralino ans stau co-annihilation is shown in Fig. (4.4).

In the scenarios where we have non-universal gaugino masses, M_1, M_2 and M_3, higgsino dominant LSP is obtained when $M_3 < M_1, M_2$, keeping m_0 lighter. This case provides us with a heaviest LSP possible up to the value of 920 Gev. However,

if sfermion mass m_0 becomes heavy, then there is a possibility for pure bino-like LSP. If we are not taking into consideration, the gaugino mass universality, then there are several ways through which the annihilation rate of a bino LSP can be enhanced. We can either increase the percentage of higgsino component by decreasing the gluino mass, or we can increase the component of wino LSP by minimizing the ratio M_1/M_2 significantly [60],[61]. If wino or gluino have mass somewhat more than mass of the bino, then bino DM is able to decipher the current DM density precisely. [62],[63],[64],[65].

The neutral wino is one of the most favorable candidates and has been studied in the prospects of indirect detection many times [61],[66],[67],[68]. If it's mass is about 3 Tev then it's abundance elegantly elaborates the observed DM density [69]. The predictions can be made from the tree level processes like

$$\chi\,\chi \;\rightarrow\; W^{+}\,W^{-},$$

where the decay of $W^{\pm}$ gives out γ-rays, cosmic rays and neutrinos. The cosmic rays generate more γ-rays as they interact with interstellar medium while transmitting through clusters of galaxies. This increases the wino annihilations even more.

4.2.1 Sensitivities to the values of $\Omega_{\chi}h^2$

The calculations of relic density are performed by implementing mSUGRA/cMSSM model for neutralinos, including co-annihilation processes. Neutralino annihilation and co-annihilation cross-sections can be calculated using different softwares [78]. Most of the parameter space is discarded at low tanβ, where the relic density value comes out to be too high. Whereas, at higher values of tanβ, there is adequate parameter space satisfied by the following equation of cold DM density [79], [80], [81]:

$$\Omega_{cdm}h^2 = 0.113 \pm 0.0034, \tag{4.1}$$

The amount of fine-tuning of SUSY parameters in order to obtain electroweak scale, increases abruptly for sparticle masses very greater than 1 Tev. While measuring this, it is better to look at the logarithmic sensitivities of the electroweak scale to

the SUSY parameters p_i:

$$D_i \equiv \frac{p_i}{m_W}\frac{\partial m_W}{\partial p_i}. \tag{4.2}$$

In our model of cMSSM, p_i includes universal soft supersymmetry breaking parameters, the common sfermion mass m_0, the universal gaugino mass $m_{1/2}$, the unified trilinear coupling parameter a_0, and the ratio of up-type and down-type Higgs vaccuum expectation value, known as tanβ. And last paramerter is the only discreet parameter i.e., the sign of μ determined by the electroweak vacuum conditions. Thus analogous measurements can be performed to quantify the sensitivity, so that relic density lies in the preferred range expressed in Eq. (4.1).

$$D_i^{\Omega} \equiv \frac{p_i}{\Omega_\chi}\frac{\partial \Omega_\chi}{\partial p_i}. \tag{4.3}$$

Now the parameters p_i contain the masses of top and bottom quark along with other cMSSM parameters introduced above. Hence the overall sensitivity for cMSSM parameter space can be written as:

$$D^{\Omega} \equiv \sqrt{\sum\nolimits_i (D_i{}^{\Omega})^2} \tag{4.4}$$

A similar measure to Eq. (4.3) has also been studied by S. F. King, and J. P. Roberts in [82]. The reason for having these studies is to achieve the accuracy in sensitivity with which the LHC is able to predict the DM. We shall find regions of parameter space, where the sensitivity parameter has very small values and conversely the regions where D^{Ω} has larger values up to 10^3. There are regions where sensitivity D_Ω is exceptionally greater, especially at large values of tanβ, where we meet the 'funnel' region and the 'focus-point' region. The funnel region in the cMSSM parameter space corresponds to rapid annihilations of $\chi\chi \to H$ [83] and the Focus point region [84] exist for relatively larger values of m_0, and lower values of $m_{1/2}$. The focus-point region is extremely sensitive to the top-mass; such that $\Omega_\chi h^2$ becomes uncertain by a large factor, when m_t is changed only at the 1% level, for any particular set of other cMSSM parameter space.

Now in order to calculate sensitivities in Eq. (4.3), we reinforce some facts. The soft independent parameters are m_0, $m_{1/2}$, a_0 and tanβ. At the electroweak scale, the gauge couplings are assumed to be unified that is considered as an input

to the RG calculations in this model parameter space. At large values of tanβ, the relic density calculations are significantly dependent upon the top and bottom quark masses and thus sensitivity to their values is also tracked. The pole mass chosen for the top-quark in the Focus-point region is, $m_t = 171\ Gev$, whereas, the bottom quark mass = 4.25 Gev [85]. At larger values of tanβ, there are numerous co-annihilation processes and diagrams that become relevant [83].

In the next four figures, the graphs are plotted in $(m_{1/2}, m_0)$ plane for fixed values of a_0, tanβ, m_t and m_b. Then their values are changed individually by small amount (about 1% increase) and the values of $\Omega_\chi h^2$ are calculated both at old and new values of each parameter. Then various sensitivities in Eq. (4.3) are calculated respective to each parameter, using these finite differences, and hence the overall sensitivity is calculated defined by Eq. (4.4). The results obtained by calculating all the differences in above mentioned parameters is quite computation-intensive than mere calculating the values of relic density. That is why the grid resolution is not intensified to expose all the fluctuations.

The region for correct value of relic density in the preferred range expressed by Eq. (4.1) is indicated by the light gray color shading, and the regions where the LSP is stau, $\tilde{\tau}$, instead of lightest neutralino, that region is indicated by red color shading. The contours of constant values of sensitivity parameter with decreasing thickness are shown in Fig. (4.5 - 4.8).

First of all, we consider the Fig. 4.5, for the following choices for parameters; tan$\beta = 10$, $\mu > 0$, $a_0 = 0$, top mass 175 Gev and bottom mass 4.25 Gev. In this plane, there are generic domains, where the moderate values $m_0/m_{1/2}$ are up to 1/3 to 2, the values of total sensitivity are also not much greater. In fact there is considerable region in this plane where the total sensitivity, $D^\Omega < 10$ or even less than 3 and we can say that for this region, there is *no need of fine-tuning of supersummetric DM*. In this generic domain, the correct value of DM relic density requires $m_{1/2}$ to be less than 400 GeV and m_0 should be less than 200 GeV. Whereas, the detailed measurements for the masses of sparticles and cMSSM parameters can be made by LHC [86].

It is obvious from Fig. (4.5), that both for very large and small values of $m_0/m_{1/2}$, sensitivity parameter, D^Ω increases. For very large values of $m_0/m_{1/2}$, the increase

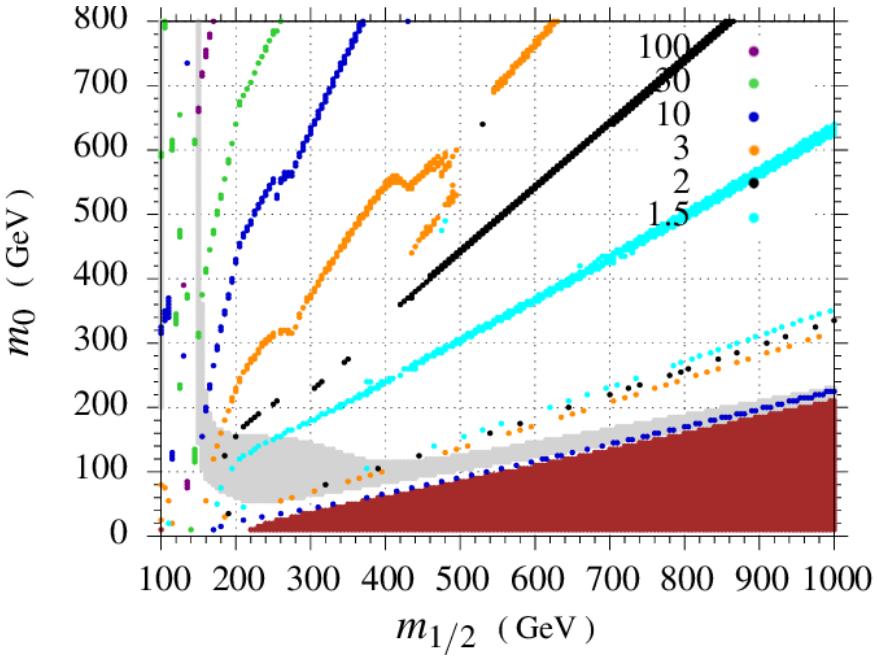

Figure 4.5: Contours of sensitivity D^{Ω} for tan$\beta = 10$, $\mu > 0$, $m_t = 175\ GeV$. Light grey region represents allowed area for relic density shown in Eq. (4.1) and dark red region is discarded due to stau LSP.

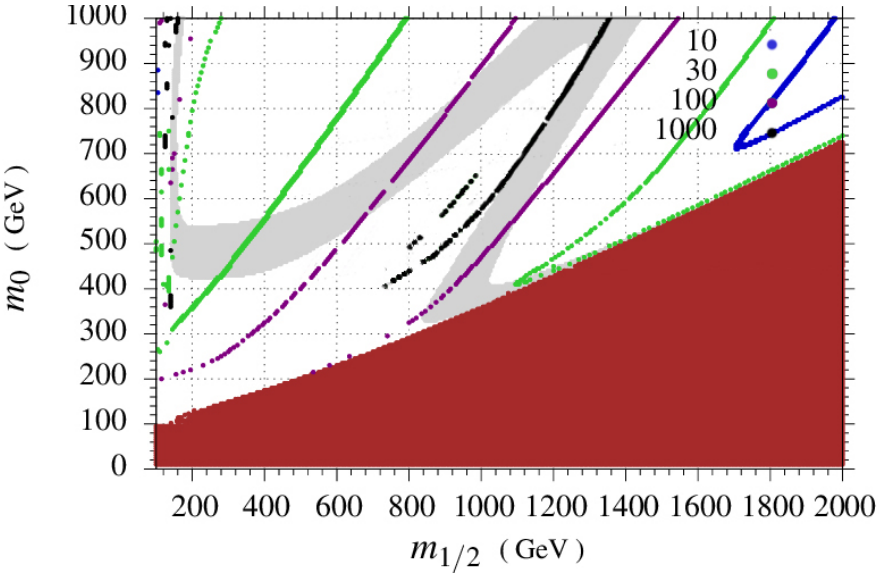

Figure 4.6: Contours of sensitivity D^{Ω} for tan$\beta = 35$, $\mu < 0$, $m_t = 175\ GeV$. Light gray region represents allowed area for relic density shown in Eq. (4.1) and dark red region is discarded due to stau LSP.

in D^{Ω} is predominately because for these regions we are approaching the annihilation cross-section channel, $\chi\,\chi \;\rightarrow\; h$ pole. (The results are shown in Fig. (4.1)). The values of relic density are lowered to a favorable and an acceptable level due to enhanced annihilation cross section for finely tuned values of $m_{1/2}$, that is why D^{Ω} exceeds the value of even, 100 in there. Getting more closer to this approach is prohibited by lower LEP bound on chargino mass and lower LEP limit on Higgs mass, $m_h > 113.5$ Gev [85]. Whereas, the increase in D^{Ω} at small $m_0/m_{1/2}$ values in the plane $(m_{1/2}, m_0)$ is because of the significance of co-annihilation [83], and this significance deviates with cMSSM parameters as well as with the difference in slepton and neutralino mass, i.e., $(m_{\tilde{l}} - m_{\chi})$. However, for this co-annihilation region, excessive fine-tuning is not required by the relic density to fit in within the preferred range, due to small D^{Ω} values. The LHC on the other side, may not entertain the detailed sparticle spectrum calculations in this region, and hence very precise values of relic density are not attained [61]. Also this region does not concur with the favorable value of $g_{\mu} - 2$ [87],[88].

Next Fig. (4.6) shows the contours for $\mu < 0$ and $\tan\beta = 35$. For this sign of μ, sensitivity contours have generally higher value than in Fig. (4.5). The region where m_0 is approximately equal to $m_{1/2}$ gives rise to the *funnel* region where the value of overall sensitivity increases rapidly, upto 100, exhibiting the significance of the direct channel annihilations of $\chi\chi \;\rightarrow\; A$ pole and hence relic density becomes smaller; A being the CP odd neutral Higgs bosons.

For higher values of $m_0/m_{1/2} \sim 2$, the measurement of sensitivity parameter D^{Ω} gives out even more uplifted values than those for $\tan\beta = 10$. This manifests that with increasing $\tan\beta$, the preferred range of m_0 also moves to a higher value and thus the *funnel* region of rapid annihilations move to higher zones of $m_0 \;\sim\; m_{1/2}$. The contours of sensitivity have almost same behavior as in Fig. (4.5), other than elevated contours now.

Funnel-region

Existence of Funnel-region is only guaranteed by the large value of $\tan\beta$, as we can see there lie no such region for smaller value of $\tan\beta$ shown in Fig. (4.5). Since this region corresponds to the A-pole region where twice of neutralino mass is

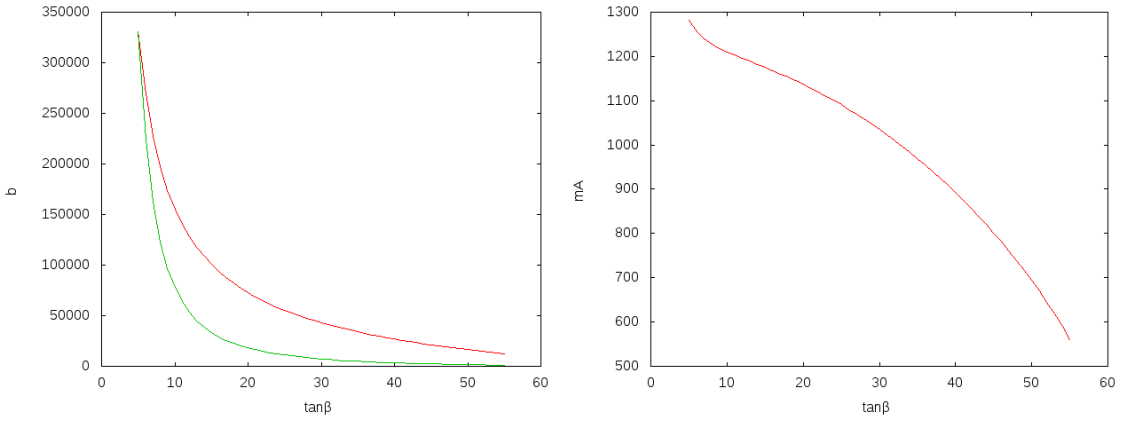

(a) Red line represents 1/tanβ curve - green curve represents b vs tanβ.

(b) Monotonically decreasing function of m_A vs tanβ .

approximately equal to m_A. In typical regions of parameter space, value of m_A is much larger than twice of neutralino mass, so the mechanism that actually make it possible, can be understood with the help of following equation;

$$m_A{}^2 = b(tan\beta + cot\beta)$$

By looking at this equation, it seems that if tanβ increases, m_A should increase further but it turns out that the parameter b which is SUSY breaking parameter, decreases largely with increasing tanβ. The behavior of m_A with increasing tanβ is shown in Fig. (4.7) where we can see that m_A is monotonically decreasing function of increasing tanβ.

Next, in Fig. (4.8) , the parameters are set for tan$\beta = 50$ and $\mu > 0$. Again for this sign of μ, there is considerable region of acceptable electroweak vacua near the upper limit. Fig. (4.8) and Fig. (4.6) have similar qualitative features in respect of the funnel region.

Finally, Fig. (4.9) displays contours for the same parameters choice as in Fig. (4.5) but now for $m_t = 171$ Gev instead of 175 GeV. This comparison for both values of top mass can be seen in Fig. (4.10). Both of these graphs are plotted for the same range of m_0 and $m_{1/2}$, which gives parallel results for $m_0 \lesssim 800$ Gev. But if we look at the upper left corner of the graphs, it is obvious that now there is more disallowed region for $m_t = 171$ GeV. This is because of the fact that since for

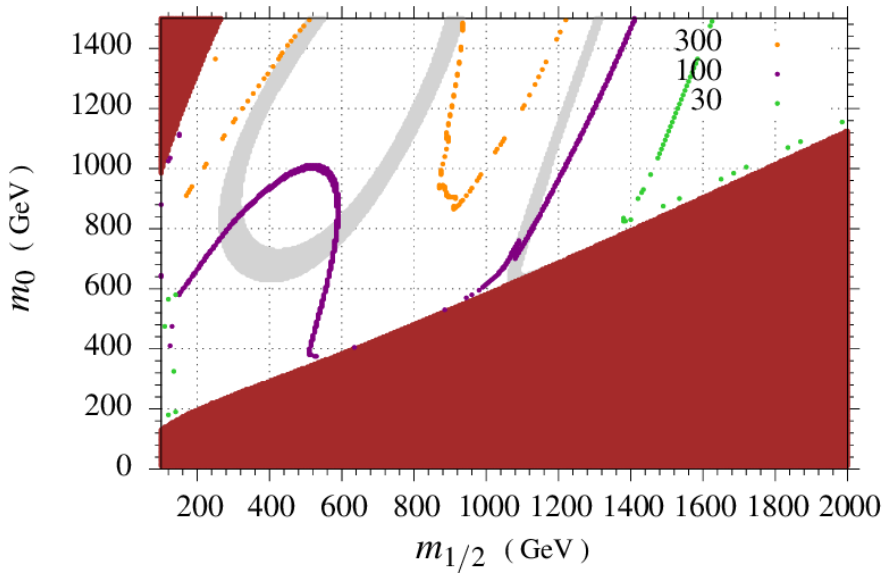

Figure 4.8: Contours of sensitivity D^{Ω} for tanβ = 50, μ >0, m_t = 175 GeV. Light grey region represents allowed area for relic density shown in Eq. (4.1) and dark red region is discarded due to stau LSP.

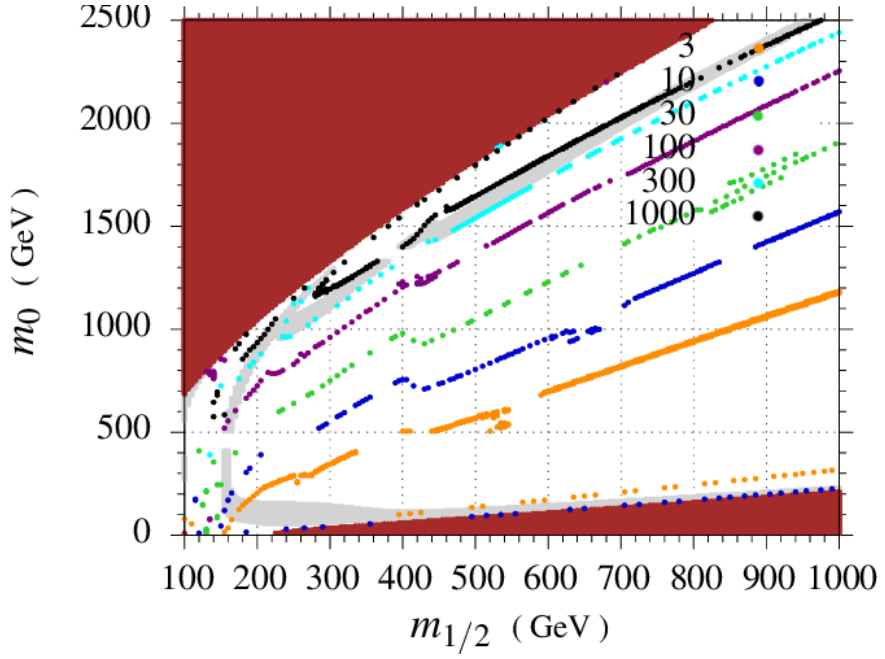

Figure 4.9: Contours of sensitivity D^{Ω} for tanβ = 10, μ >0, m_t = 171 GeV. Light gray region represents allowed area for relic density shown in Eq. (4.1). The upper Dark red region is discarded due to electroweak vacuum conditions and lower dark red region is disallowed due to stau LSP.

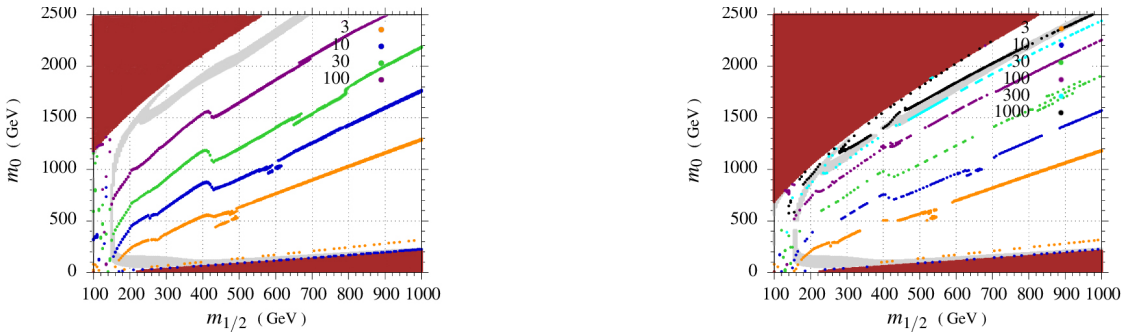

Figure 4.10: $\tan\beta = 10$, $\mu > 0$, $A_0 = 0$, on left $m_t = 175$ GeV and on right m_t =171 GeV

radiative electroweak symmetry breaking (REWSB) both the Higgs mass parameters, $m_{H_u^2}$ and $m_{H_d^2}$ are chosen to be positive at the GUT scale and they acquire negative sign through radiative running of the coupling while running down to the electroweak scale. This is because of the effect of large top Yukawa coupling seen clearly in renormalization group equation for $m_{H_u^2}$, i.e.,

$$\frac{dm_{H_u}^2}{dt} = -[3(g_2 M_2^2 + \tfrac{1}{5} g_1 M_1^2) - 3Y_U(\tilde{m}_Q^2 + \tilde{m}_U^2 + m_{H_2}^2 + A_U^2)]$$

Here in this equation, we can see two contributions, one is negative due to gauge type interaction and positive contribution is due to Yukawa interaction. However the correct sign for this equation has to be positive, only then $m_{H_u^2}$ and $m_{H_d^2}$ will be negative at the low scale. Decreasing top mass also decreases Yukawa interaction and thus condition of REWSB is not met easily and so there is more disallowed region in this case.

Also m_0 and $m_{1/2}$ plotted for this range can allow us to see *Focus Point* region for $m_0 \gtrsim 1000$ Gev. This region extends to join the upper dark red shaded region where electroweak vacuum is not consistent. The increased values of contours of $D^{\Omega} \sim 1000$ are well defined by the fact that the *Focus Point* region is very sensitive to the top mass. (Similar behavior of high sensitivities to m_t could be seen in fourth paper of reference [87]).

Plots of individual sensitivities

The variations in the overall sensitivity parameter can be better understood

by plotting the individual values of D_i^{Ω} for various illustrative choices of cMSSM parameter space against the constant values of m_0 or $m_{1/2}$. The contour of sensitivity to a_0 has no reasonable effect on changing other parameters and is not shown in any of the following plot.

The parameters in the Fig (4.11) are set as: $\tan\beta = 10$, $a_0 = 0$, $\mu > 0$, $m_0 =$ 100 Gev, while m_t= 175 Gev and bottom mass is set as 4.25 Gev, corresponding to the Fig. (4.5). The dominant sensitivities D_i^{Ω} in the domain where $150 \lesssim m_{1/2} \lesssim 500$ are those of m_0 and $m_{1/2}$ followed by the sensitivity of m_t. Lastly there are sensitivities, which are almost negligible in this zone, related to m_b, $\tan\beta$ and a_0. For $m_{1/2} \lesssim 150$ Gev, there are rapid soaring peaks of some of D_i^{Ω}. In this zone, as the neutralino mass travels across the value $m_h/2$ and the annihilation rate of $\chi\chi \rightarrow h$ alters significantly we can see the dominating peaks of sensitivity D_i^{Ω} to m_t and m_0 that can be seen in Fig. (4.11). The DM problem is not concerned to this pole region, because due to the LEP constraints on charginos, this region is excluded and it offers very suppressed values of relic density, i.e., $\Omega_\chi h^2 << 0.1$. As the stau-neutralino co-annihilation region is approached, for $m_{1/2} \gtrsim 400\ GeV$ shown in Fig. (4.12) there is sharp rise in sensitivity to m_0. The rise in sensitivity is not followed by the fall because the disallowed region due to $\bar{\tau}$ LSP follows next. Since m_0 and $m_{1/2}$ are the key parameters in controlling the mass difference of $m_\chi - m_{\tilde{\tau}}$, thus their sensitivities are also expected to be greater and due to the robust dependence of m_χ on $m_{1/2}$ and $m_{\tilde{\tau}}$ on both of m_0 and $m_{1/2}$. It is clear from the Fig. (4.11) that none of the individual sensitivity in this region exceeds the value of 10, since the combined sensitivity in this region for Fig. (4.5) also shows $D^{\Omega} \lesssim 20$ for $\tan\beta = 10$.

Next, in the Fig. (4.14), contours for fixed $m_0 = 400$ Gev, $\tan\beta = 50$ and $\mu > 0$, are shown which corresponds to a slice of parameter space in Fig. (4.6). The region for $m_{1/2} \lesssim 150$ Gev has rapid soaring peaks of different sensitivities because this is the pole region. In this region, for $m_{1/2} \lesssim 600$ Gev, the most dominant sensitivity through out, is that of m_t, where we meet the funnel region.

From Fig. (4.15), it can be seen clearly that annihilation region where, $\chi\chi \rightarrow H, A$ region, starts from 500 GeV $\lesssim m_{1/2} \lesssim$ 650 GeV, for which we see peak of sensitivity to m_t in upper figure.

Next, a slice corresponding to the Fig. (4.8) is shown in Fig. (4.16) for fixed

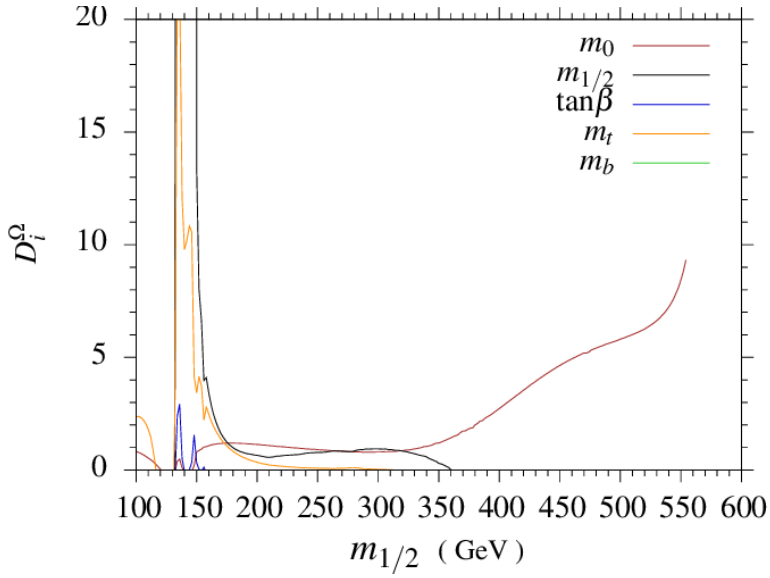

Figure 4.11: Fine-tuning sensitivities D_i^Ω to different input parameters are plotted in different colors for $m_0 = 100$ GeV, (a) tan$\beta = 10$, $\mu > 0$ and $m_t = 175\ GeV$.

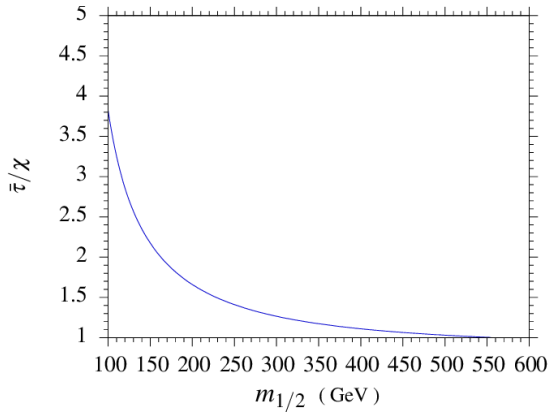

Figure 4.12: Stau-neutralino co-annihilation region.

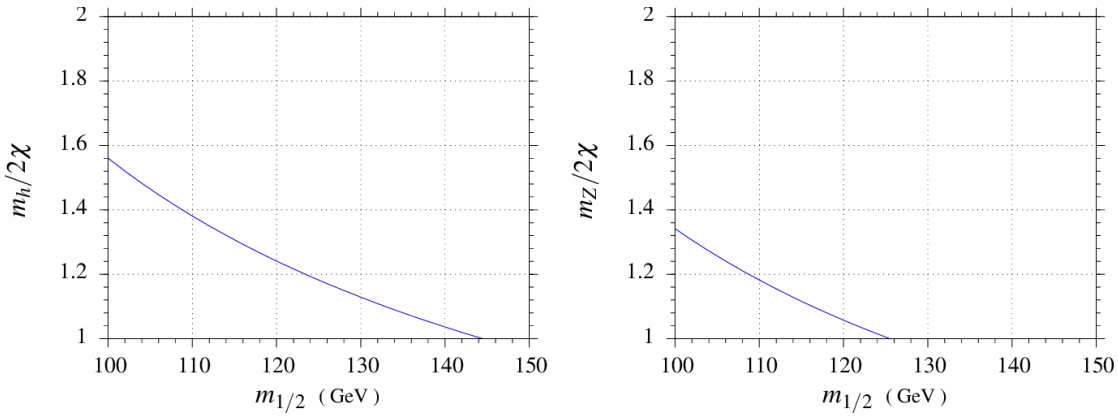

(a) Light-Higgs annihilation region. (b) Z-pole annihilation region.

Figure 4.13: Annihilation regions for $m_{1/2}$ <150 GeV.

m_0 = 1000 Gev and tanβ = 50, μ >0, a_0=0, m_t = 175 and m_b same as before 4.25 GeV. The sensitivity to m_t is the most dominant one as the funnel approaches at about $m_{1/2} \gtrsim 900$ GeV. Also the sensitivity to tanβ has sharp increase as well. All of these have a rapid increase as we proceed towards the funnel. For the co-annihilation region at about $m_{1/2} = 180$ GeV, the increase in sensitivities is due to the importance of $m_{\tilde{\tau}} - m_\chi \to 0^+$. In the last we have Fig. (4.16) corresponding to the Fig. (4.9) , this time for fixed $m_{1/2} = 250$ Gev and varying m_0, tanβ = 10, $\mu > 0$ and $m_t = 171$ GeV. For this choice of parameters, we cut through the focus point region. Here it can be seen that as we proceed towards focus point region, there is a very sharp increase in the sensitivity to m_t. Both m_0 and $m_{1/2}$ sensitivity values are greater in this plane up to 10 Tev, showing the narrower strip of focus point region. At smaller $m_{1/2}$, the sensitivities are invisible in the generic domain of this plot, but are almost like those shown in Fig. 4.11.

The importance of Focus-point region can be understood with the help of Table 4.1, where it can be seen clearly that for points close to this region value of $\Omega_\chi h^2 \to 0$ and the Higgsino component of LSP is dominant as compared to bino-component of LSP and $\mu \to 0$. The bino-component increases as we move away from Focus point region.

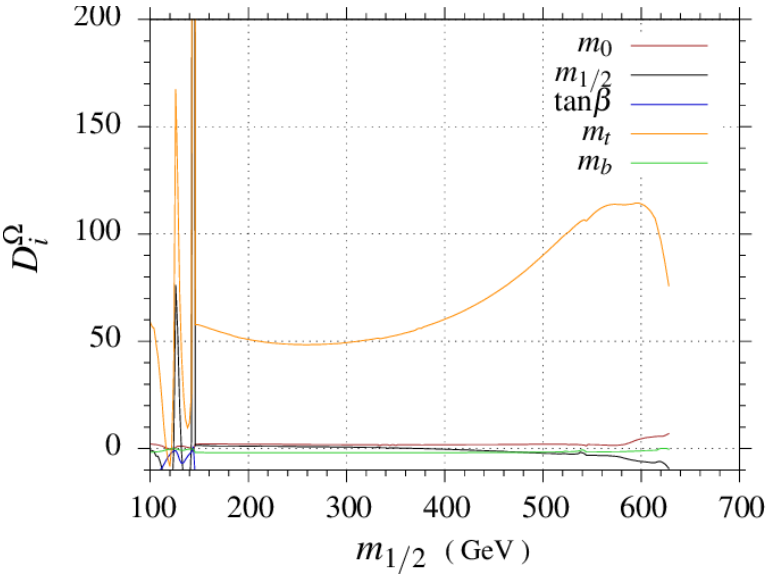

Figure 4.14: Fine-tuning sensitivities D_i^Ω to different input parameters are plotted for $m_0 = 400$ GeV, tan$\beta = 50$, $\mu > 0$ and $m_t = 175\ GeV$.

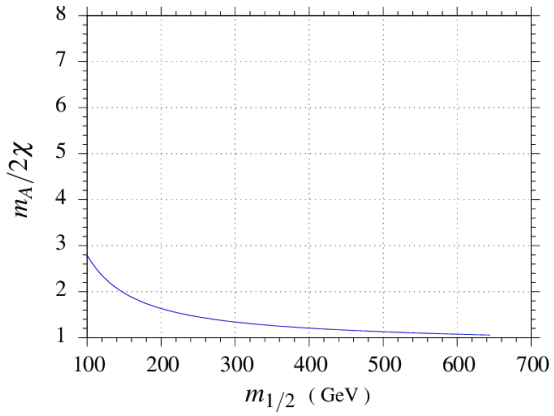

Figure 4.15: m_A pole annihilation region.

m_0	$m_{1/2}$	Ω_{h^2}	m_χ	m_h	m_A	bino-comp	higgsino-comp	μ values
1220	265	0.00024731	43.3108	110.737	1211.47	0.371281	0.908021	74.7519
1220	270	0.00011922	54.3961	110.729	1212.93	0.425806	0.886005	89.2653
1220	275	0.0617881	64.5577	110.735	1214.51	0.483256	0.857663	103.128
1220	280	0.123618	73.5424	110.743	1216.16	0.541016	0.823693	116.037
1220	285	0.0421836	81.4584	110.755	1217.86	0.597484	-0.112292	128.132
1220	290	0.0405287	88.437	110.771	1219.62	0.650944	-0.106325	139.551
1220	295	0.0393717	94.6066	110.788	1221.41	0.699883	-0.1012	150.409
1220	300	0.0442503	100.088	110.808	1223.24	0.743282	-0.0967253	160.797
1220	305	0.0536456	104.992	110.83	1225.12	0.780728	-0.0927705	170.775
1220	310	0.0667049	109.422	110.853	1227.02	0.81243	-0.0892345	180.429
1220	315	0.0844621	113.468	110.878	1228.96	0.838941	-0.0860431	189.781
1220	320	0.10984	117.201	110.904	1230.94	0.860924	-0.0831434	198.869
1220	325	0.143226	120.681	110.93	1232.95	0.87911	-0.0804918	207.723

Table 4.1: Points close to Focus Point region, $m_t = 171$ GeV and tab$\beta = 10$.

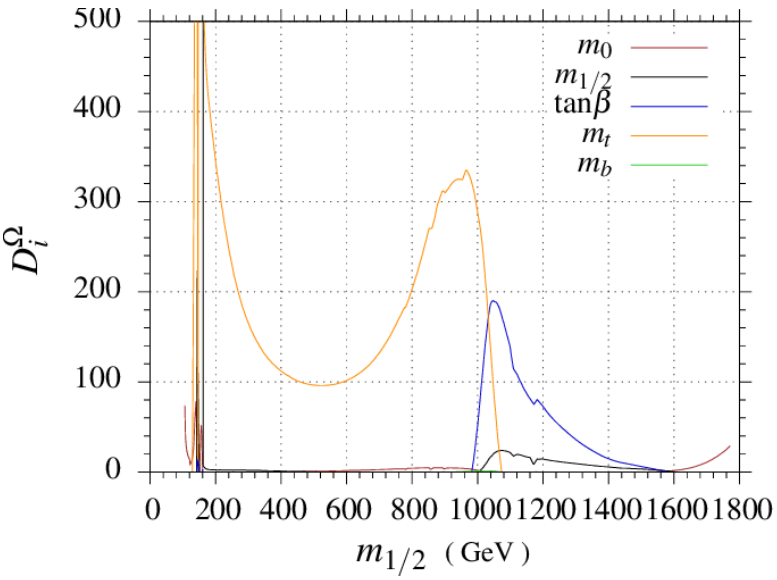

Figure 4.16: Fine-tuning sensitivities D_i^Ω to different input parameters are plotted in different colors for $m_0 = 1000$ GeV, tan$\beta = 50$, $\mu > 0$ and $m_t = 175\ GeV$.

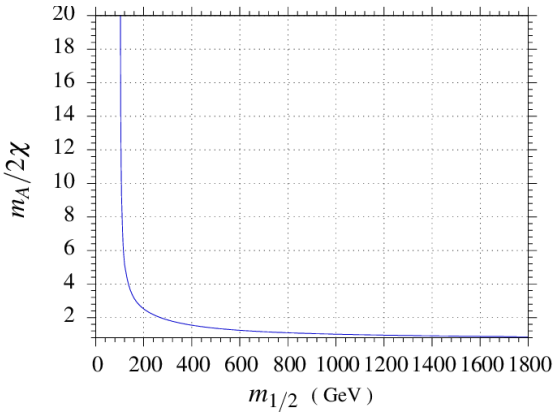

Figure 4.17: m_A pole annihilation region corresponding to Fig. (4.16).

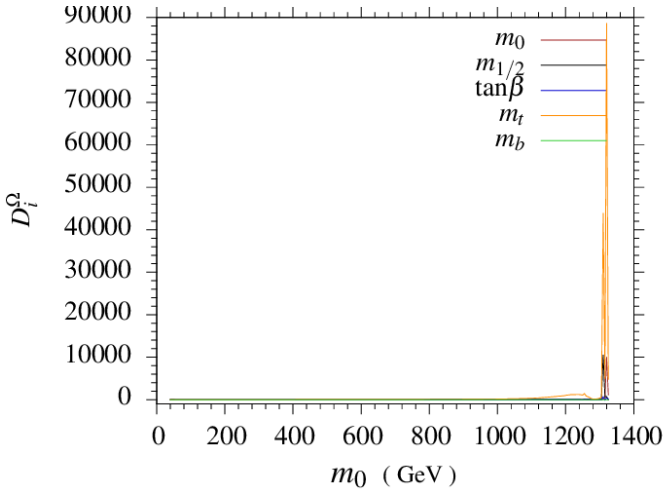

Figure 4.18: Fine-tuning sensitivities D_i^Ω, to different input parameters are plotted in different colors for tan$\beta = 10$, $\mu > 0$ and $m_t = 171\ GeV$.

Chapter 5

Concluding Remarks

Since standard model does not suggest any viable candidate for dark matter, in this review work, dark matter relic densities are investigated in a suitable supersymmetric standard model, constrained minimal supersymmetric standard model (cMSSM). Keeping in mind, the value of relic density of dark matter measured observationally by Planck satellite experiment, we are able to suggest a suitable candidate, i.e. neutralino, for dark matter that fulfills the requirements of cold dark matter candidate.

The sensitivities to the parameters of cMSSM are calculated. There are different regions that appeared in the parameter space corresponding to low and high values of relic density. Annihilation and co-annihilation are important channels that help to get correct value of dark matter relic density for certain choice of parameters.

These regions include stau-neutralino co-annihilation region for smaller values of m_0, where stau and neutralino are quasi degenerate in mass. As the value of m_0 is increased, the annihilation cross section rate is suppressed with the increase in slepton masses, and thus the relic density values are also raised up.

Further increase in the values of m_0 beyond the level of 1 TeV, the higgsino component of the neutralino increases as the parameter μ falls, hitting the Focus Point region. In this region the annihilation rate enhances through the scattering of WW, ZZ, hh and Zh which increases further as the values of m_0 are increased. Now finally, $|\mu| \rightarrow 0$, for large values of m_0 and radiative electroweak symmetry breaking can no longer occur.

It is also shown that there are 'generic' domains in the cMSSM parameter space for moderate values of tanβ, where the values of overall sensitivity of relic density are rather small. For the generic regions, where we attain $\Omega_\chi h^2$ in the range preferred by cosmology and Astrophysics, there is no need of 'fine-tuning' of the cMSSM parameters.

At larger values of tan$\beta > 30$, we have uplifted values of sensitivities because of the A-pole Funnel-region occurring at about $m_0 \sim m_{1/2}$. Also it is seen that small to moderate values of tanβ in the calculations reveal no novel results.

In the last, plots of individual sensitivities have been plotted to help understand which parameters are contributing for finely tuned regions.

Bibliography

[1] S. Underwood "Supersymmetric Dark Matter in the NMSSM and E6SSM "*Phys. Rev. Lett.*, **13** (2016) 321-323.

[2] J. Frieman, M. Turner and D. Huterer, Ann.Rev. Astron. "Dark Energy and the Accelerating Universe ", *Ann.Rev.Astron.Astrophys.*, **46** (2008) 385-432.

[3] E. Komatsu et. al. "Seven-Year Wilkinson Microwave Anisotropy Probe (WMAP) Observations: Cosmological Interpretation ", *Astrophys. J. Suppl.*, **192** (2011).

[4] "Planck Collab. 2015 Results I, Overview of products and scientific results",*Astron. and Astrophys.*, arXive:1502.01582v2.

[5] "Planck Collab. 2015 Results XIII ", *Astron. and Astrophys.*, arXive:1502.01589v2.

[6] Image from http://map.gsfc.nasa.gov/, Wilkinson Microwave Anisotropy Probe.

[7] U. Amaldi, W. de Boer and H. Fiirstenau, "Unification of Couplings "*Phys. Lett. B*, **260** (1991) 447-455.

[8] A. Kusenko and M. E. Shaposhnikov, "Supersymmetric Q-balls as dark matter "*Phys. Lett. B*, **418** (1998) 46-54.

[9] A. Signer, "abc of SUSY ", *J. Phys. G* **36** (2009) 1-37.

[10] D. I. Kazakov, "Beyond the standard model (in search of supersymmetry) ", (2001).

[11] F. Zwirner, "Some New Aspects of Supersymmetry R-Parity Violating Interactions "*Phys. Lett. B* **132** (1983) 103-106.

[12] R. Kuchimanchi and R.N. Mohapatra, "No parity violation without R-parity violation "*Phys. Rev. D* **48** (1993) 4352.

[13] G. Jungman, M. Kamionkowski and K. Griest,"Supersymmetric Dark Matter", *Phys. Rept.* **267** (1996) 195-373.

[14] P. W. Higgs, "Broken symmetries, massless particles and gauge fields",*Phys. Lett.* **12** (1964) 132-133.

[15] P. W. Higgs, "Broken Symmetries and the Masses of Gauge Bosons", *Phys. Rev. Lett.* **13** (1964) 508-509.

[16] G. S. Guralnik, C. R. Hagen, and T. W. B. Kibble, "Global Conservation Laws and Massless Particles", *Phys. Rev. Lett.* **13** (1964) 585-587.

[17] P. W. Higgs, "Spontaneous Symmetry Breakdown without Massless Bosons", *Phys. Rev.* **145** (1966) 1156-1163.

[18] F. Englert and R. Brout, "Broken Symmetry and the Mass of Gauge Vector Mesons", *Phys. Rev. Lett.* **13** (1964) 321-322.

[19] Debasish Majumdar, *Dark Matter; An Introduction*, 2015, 69-237.

[20] Steven Weinberg, *The First Three Minutes.*, 1993, 44-122.

[21] C.L. Bennett et al. "WMAP Collaboration", *Astrophys. J. Suppl.* **148**, (2003).

[22] C. Bennette et al., "Seven-Year Wilkinson Microwave Anisotropy Probe WMAP Observations", *Astrophys. J. Supp.* **208** (2013) 20-48.

[23] P.A.R. Ade et al. "Planck 2013 results. XVI. Cosmological parameters", *astro-ph.CO*.

[24] M.S. Turner: "Cosmological Parameters, In Particle Physics and the Universe", ed. by D. Caldwell, AIP conference proceedings, *Astrophys. J. Supp.* **478** (1999) 113-128.

[25] J.R. Primack, "Status of Cosmology. In Cosmic Flows: Towards an Understanding of Large-Scale Structure, ed. by S. Courteau, M.A. Strauss, J.A. Willick (ASP Conference Series)", *astro-ph* (1999).

[26] Ostlie and Carroll, *An Introduction to Modern Astrophysics* (2007) 1192-1194.

[27] "First Year Wilkinson Microwave Anisotropy Probe (WMAP) Observations: Determination of Cosmological Parameters", *Astrophys. J. Supp.* (2003).

[28] "Constraints on cosmological parameters from MAXIMA-1", *Astro. Phys* **545** (2000) L1L4.

[29] "Big Bang Nucleosynthesis predictions for precision cosmology" *Astro. phys.* **552** (2001) L1L5.

[30] "Cosmological implications of the MAXIMA-1 High-Resolution cosmic microwave background anisotropy measurement", *Astro. phys.* **561** (2001) L7L10.

[31] A. H. Gonzalez, D. Zaritsky, and A. I. Zabludoff, "A census of baryons in galaxy clusters and groups", *Astro. Phys.* (2007) **666** 147-155.

[32] Croswell, Ken, "The Universe at Midnight", Simon and Schuster, p. 165. (2002).

[33] Udated Nov 2015, by O. Lahav (University College London) and A. R. Liddle (University of Edinburgh), "THE COSMOLOGICAL PARAMETERS", *Chin. Phys. C* **40** 386-392.

[34] S. van den Bergh, "The Early History of Dark Matter", *Astro. Phys.* **111** (1999) 657-660.

[35] V. Trimble, *Ann. Rev. Astron. Astrophys.* **25** (1987) 425-472.

[36] G. Bertone and D. Hooper "A History of Dark Matter" *Astro. phys. HE* (2016) 157-229.

[37] P. Ostriker and P. J. E. Peebles, "A Numerical Study of the Stability of Flattened Galaxies: or, can Cold Galaxies Survive?" *Astro. Phys.* **186** (1973) 467-480.

[38] J. P. Ostriker, P. J. E. Peebles, and A. Yahil,"The size and mass of galaxies, and the mass of the universe"*Astro. Phys.* **193** (1974) L1-L4.

[39] P. Nath, R. Arnowitt, and A. Chamseddine, "Lepton and Baryon Number Violation in Particle Physics", *Nucl. Phys.B* **227** (1983) 121-133.

[40] L. Bergstrom, "Non-Baryonic Dark Matter - Observational Evidence and Detection Methods"*Rept. Prog. Phys.* **63** (2000) 793-852.

[41] G. Bertone, D. Hooper and J. Silk, "Particle Dark Matter: Evidence, Candidates and Constraints"*Phys. Rept.* **405**, (2005) 279-390.

[42] M. Kamionkowski, "Dark Matter and Dark Energy", *Astro.phys.* **614** (2004) 186-239.

[43] G. Bertone (ed.), *Particle Dark Matter, Cambridge University Press* (2009) 3-12.

[44] K.Freeman, G. Mcnamra *In Search of Dark Matter*, (2006), 83-145.

[45] K.G. Begeman, A.H. Broeils, R.H. Sanders, 'Extended rotation curves of spiral galaxies '*ISSN 0035-8711* **249** (1991) 523-537.

[46] F. S. Queiroz "Dark Matter Overview: Collider, Direct and Indirect Detection Searches"*hep-ph* (2016) 1605-1625.

[47] P. Picozza, L. Marcelli, O. Adriani, et al., "American Institute of Physics Conference Series", **1166** (2009) 141-150.

[48] M. G. Aartsen, K. Abraham "The IceCube Collaboration", *Astro. Phys* 34th International Cosmic Ray Conference (2015).

[49] "ANTARES Collaboration, JCAP 11", *Astro. Phys.* **032** (2013).

[50] "First Dark Matter Search Results from XENON1T, 29th Rencontres de Blois on Particle Physics and Cosmology, Blois, Loire Valley, France"(2017).

[51] http://lss.fnal.gov/archive/2005/conf/fermilab-conf-05-438-e.pdf "Current and Future Searches for Dark Matter"(conference paper).

[52] G. R. Farrar and P. Fayet. "Phenomenology of the production, decay, and detection of new hadronic states associated with supersymmetry", *Phys. Lett., B* **76 575** 1978 575-579.

[53] E. Cremmer et al. "SuperHiggs effect in supergravity with general scalar interactions", *Phys. Lett., B* **79** (1978) 231-234.

[54] E. Cremmer et al. "Spontaneous symmetry breaking and Higgs effect in supergravity without cosmological constant", *Nucl. Phys. B* **147** (1979) 105-131.

[55] K. Griest and D. Seckel, "Three exceptions in the calculation of relic abundances" *Phys. Rev. D* **43** (1991) 3191-3210.

[56] J. Ellis, T. Falk, K. Olve, and M. Srednicki, "Calculations of Neutralino-Stau Coannihilation Channels and the Cosmologically Relevant Region of MSSM Parameter Space." *Astropart. Phys.* **13** (2000) 181-213.

[57] R. Arnowitt, B. Dutta, and Y. Santoso, "Coannihilation Effects in Supergravity and D-Brane Models" *Nucl. Phys. B* **606** (2001) 59-83.

[58] M. Gomez, G. Lazarides, and C. Pallis, "Supersymmetric Dark Matter Detection at Post-LEP Benchmark Points" *Phys. Lett. B* **487**, (2000) 313-317.

[59] L. Roszkowski, R. Ruiz de Austri and T. Nihei, "Phenomenological constraints on patterns of supersymmetry breaking" *Phys. Lett. B* **024** (2001) 162-172.

[60] A. Birkedal-Hansen and B. Nelson, "Increasing the neutralino relic abundance with slepton coannihilations: consequences for indirect dark matter detection" *Phys. Rev. D* **64** (2001) 326-334.

[61] H. Baer, A. Mustafayev, E. Park and S. Profumo, "Probing SUSY beyond the reach of LEP2 at the Fermilab Tevatron" *High Energy Phys.* **0507** (2005) 046.

[62] H. Baer, T. Krupovnickas, A. Mustafayev, E.-K. Park, S. Profumo, et al., "New probes for bino dark matter with coannihilation at the LHC", *Hep. Phys.* **011** (2005) arXiv:hep-ph/0511034 [hep-ph].

[63] S. Profumo and C. Yaguna, "Probing Bino-Gluino Coannihilation at the LHC", *Phys.Rev.D* **69** 115009 (2004).

[64] D. Feldman, Z. Liu, and P. Nath, "Gluino NLSP, Dark Matter via Gluino Coannihilation, and LHC Signatures" *Phys.Rev.D* **80**, 015007 (2009).

[65] A. De Simone, G. F. Giudice, and A. Strumia, "Wino-like Minimal Dark Matter and future colliders", *Hep. Phys.* **081** (2014).

[66] U. Chattopadhyay, D. Das, P. Konar, and D. Roy, "Minimal Asymmetric Dark Matter" *Phys.Rev.D* **75** 073014 (2007).

[67] P. Ullio, "Indirect detection of neutralino dark matter candidates in anomaly-mediated supersymmetry breaking scenarios" *Hep. Phys.* **053** (2001),hep-ph/0105052, URL http://arxiv.org/abs/hep-ph/0105052.

[68] P. Grajek, G. Kane, D. J. Phalen, A. Pierce, and S. Watson "Dark matter prospects in deflected mirage mediation"(2008).

[69] J. Hisano, S. Matsumoto, M. Nagai, O. Saito, and M. Senami, "Non-perturbative Effect on Thermal Relic Abundance of Dark Matter" *Phys.Lett.B* **646** (2007) 34-38.

[70] A. Chamseddine, R. Arnowitt, and P. Nath, "Non-perturbative Effect on Thermal Relic Abundance of Dark Matter" *Phys. Rev.Lett.* **49** (1982) 970-972.

[71] P. Nath, R. Arnowitt, and A. Chamseddine, "Locally supersymmetric grand unification" *Nucl. Phys.B* **227** (1983) 121-133.

[72] N. Ohta, "Grand Unified Theories Based on Local Supersymmetry" *Prog. Theor. Phys.* **70** (1983) 542-549.

[73] L. Hall, J. Lykken, and S. Weinberg, "Proton decay in locally supersymmetric GUT" *Phys. Rev. D* **27** (1983) 317-332.

[74] R. Arnowitt and P. Nath, "Proton decay in locally supersymmetric GUT"Supersymmetric mass spectrum in SU(5) supergravity grand unification*Phys. Rev. Lett.* **69** (1992) 725-733.

[75] G. Ross and R. Roberts, "LIGHT NEUTRALINOS IN B-DECAYS" *Nucl. Phys. B* **377** (1992) 571-921.

[76] B.C. Allanach, Comput. Phys. Commun. **143** (2002) 305-331.

[77] "micromegas"G. Blanger, F. Boudjema, A. Pukhov, A. Semenov, *Comput.Phys.Commun.*, **192** (2015) 322.

[78] CompHEP v.33.23, by A. Pukhov et al., "Relic density of neutralinos in minimal supergravity"(1999) hep-ph/9908288.

[79] D. N. Spergel et al. [WMAP Collaboration], "First Year Wilkinson Microwave Anisotropy Probe (WMAP) Observations: Determination of Cosmological Parameters" *Astrophys.J.Suppl.* **170** (2007) 377-468.

[80] A. E. Lange et al.[Boomerang Collaboration], "First Estimations of Cosmological Parameters From BOOMERANG" *Phys. Rev. D* **63** 042001 (2001).

[81] A. Balbi et al., "Constraints on Cosmological Parameters from MAXIMA-1" *Astrophys. J.* **545** (2000) L1-L4.

[82] S. F. King, and J. P. Roberts "Natural Implementation of Neutralino Dark Matter", (2006).

[83] J. Ellis, T. Falk, G. Ganis, K. A. Olive and M. Srednicki, "The CMSSM Parameter Space at Large tan beta" *Phys.Lett.B* **510** (2001) 236-246.

[84] J. L. Feng, K. T. Matchev and T. Moroi, "Hadron Collider Physics 2005" *Phys. Rev. Lett.* **84** (2000) 2322-2325.

[85] P. Abreu et al., DELPHI collaboration, "Search for the standard model Higgs boson at LEP" *Phys. Lett. B* **499** (2001) 23-37.

[86] I. Hinchliffe, F. E. Paige, M. D. Shapiro, J. Soderqvist and W. Yao, "Particle components of dark matter" *Phys. Rev. D* **55** (1997) 5520-5540.

[87] J. Ellis, D. V. Nanopoulos and K. A. Olive, "Combining the Muon Anomalous Magnetic Moment with other Constraints on the CMSSM" *Phys.Lett.B* **508** (2001) 65-73.

[88] H. N. Brown et al., "Final Report of the Muon E821 Anomalous Magnetic Moment Measurement at BNL Muon g 2 Collaboration", *Phys. Rev. Lett.* **86** (2001) 2227-2231.